

First-Principle Coarse-Graining Framework for Scale-Free Bell-Like Association and Dissociation Rates in Thermal and Active Systems

Josip Augustin Janeš,^{1,2} Cornelia Monzel³,[✉] Daniel Schmidt,^{2,4} Rudolf Merkel,⁵ Udo Seifert^{3,4},[✉] Kheya Sengupta,⁶ and Ana-Sunčana Smith^{2,1,*}

¹Group for Computational Life Sciences, Ruđer Bošković Institute, Zagreb, Croatia


²PULS Group, Department of Physics, FAU Erlangen-Nürnberg, IZNF, Erlangen, Germany

³Experimental Medical Physics, Department of Physics, Heinrich-Heine Universität Düsseldorf, 40225 Düsseldorf, Germany

⁴II. Institut für Theoretische Physik, Universität Stuttgart, 70550 Stuttgart, Germany

⁵Institute of Biological Information Processing 2: Mechanobiology, Forschungszentrum Jülich GmbH, 52425 Jülich, Germany

⁶Centre Interdisciplinaire de Nanoscience de Marseille (CINaM), CNRS, Aix Marseille University, 13009 Marseille, France

 (Received 27 April 2021; revised 21 March 2022; accepted 28 June 2022; published 22 August 2022)

Fluctuations of surfaces that harbor reactive molecules interacting across the intervening space strongly influence the reaction kinetics. One such paradigmatic system is the cell membrane, with associated proteins, binding to an interior or an exterior scaffold—for example, the cytoskeleton in the former and the extracellular matrix in the latter case. Given that membrane fluctuations are significant and regulated by the activity of the cell, we hypothesize that these active fluctuations can be tuned to influence ligand-receptor-mediated adhesion. However, a comprehensive model, deriving both binding and unbinding rates from first principles, has not yet been established, and as such, the effect of the membrane activity on the rates remains an open problem. Here, we solve this issue by establishing a systematic coarse graining procedure, providing a cascade of expressions for rates appropriate for the observed timescale, and present a scale-free formulation of rates. In the first step, we introduce a minimal model to recover the so-called Bell-Dembo rates from first principles, where the binding and unbinding rates depend on the instantaneous position of the membrane. We then derive the analytical coarse-grained rates for thermal fluctuations, recovering a result that has previously been successfully used in the literature. Finally, we expand this framework to account for active fluctuations of the membrane. In this step, we develop a mechanical model that convolutes Gauss and Laplace distributed noise. This choice may have universal features and is motivated by our analysis of measurements in two very different cell types, namely, human macrophages and red blood cells. We find that cell activation enables the formation of bonds at much larger separations between the cell and the target. This effect is significantly greater for binding to a surface on the extracellular compared to the intracellular side. We thus show that active fluctuations directly influence protein association and dissociation rates, which may have clear physiological implications that are yet to be explored.

DOI: [10.1103/PhysRevX.12.031030](https://doi.org/10.1103/PhysRevX.12.031030)

Subject Areas: Biological Physics, Soft Matter, Statistical Physics

I. INTRODUCTION

The plasma membrane of a biological cell is never at rest. Driven by thermal noise and by biological activity, its shape

is constantly experiencing rapid oscillations with amplitudes of up to a couple hundred nanometers [1]. The thermal component of the membrane spectrum has been extensively studied, and a full theoretical foundation has been established over the years [2–7]. It is set by thermodynamic conditions such as temperature and pressure, and can be altered locally by modifications of the membrane material properties or the introduction of constraints.

On the other hand, the active component of fluctuations, albeit clearly identified [8], is significantly less well understood. The relationship between the responsible biological processes and the stochastic excitations of the

*Corresponding author.

ana-suncana.smith@fau.de; asmith@irb.hr

Published by the American Physical Society under the terms of the [Creative Commons Attribution 4.0 International license](https://creativecommons.org/licenses/by/4.0/). Further distribution of this work must maintain attribution to the author(s) and the published article's title, journal citation, and DOI.

membrane is still subject to debate [8,9]. The proposed sources of activity include conformational changes of channels and pumps occurring during molecular transport [10], membrane-actin interactions [11,12], membrane-embedded motors [13], and curvature-inducing [14–16] and thickness-composition changing [17] protein-membrane interactions, among other possibilities.

As the membrane plays an important functional role in cells, it is no surprise that the nature of its fluctuations has an effect on many cellular processes. Notably, it is recognized that thermal membrane fluctuations can affect the kinetics and affinity of membrane adhesion receptors [18–22]. Thus, actively modifying membrane fluctuations could serve as an efficient tool for dynamic regulation of membrane receptor kinetics, a feature that could be exploited by the cell for localized control of its interactions with the environment. Indeed significant spatiotemporal variability of active fluctuations has been shown to exist in different cells [23]. Moreover, the local coupling between active fluctuations and cell adhesion has been reported in several cellular systems [24,25], hinting at the role of active fluctuations in regulating the formation of cadherin bonds. Similarly, macrophage activation with cytokine interferon gamma ($\text{IFN}\gamma$) reflects in the increase of both the membrane activity [23,26] and the Fc receptor avidity [27], hinting at the causal relation between the two.

The above considerations beg for a better experimental and theoretical understanding of the interplay between membrane fluctuations and receptor kinetics.

The current theory of active membranes is usually based on specific mechanistic models expressed typically by a set of stochastic equations with the appropriate noise correlations (for a review of active models, see Ref. [9]). However, even for some of the most studied systems, such as the RBCs, for which the membrane activity has been well studied and experimentally confirmed [8,28], the main source of activity is still debated. The situation is even more obscured as the structural complexity of cells increases. Moreover, it would not be surprising if the exact mechanistic processes behind activity vary across different types of cells, mirroring the differences in their mechanistic and chemical structure. Consequently, commitment to specific sources of membrane activity during modeling severely restricts the applicability of the derived fluctuation model. Hence, there is a need for a unifying modeling principle that would enable the construction of a general, cell-type-independent framework for ligand-receptor binding in membranes.

If unconstrained, ligands and receptors bind following a lock-and-key principle, characterized by the so-called intrinsic rate, over a reaction coordinate that relies on structural complementarity of the receptor for its ligand. However, confinement of the receptor to the membrane that maintains a separation from the ligand introduces constraints (Fig. 1).

The first constraint to consider is the role of confinement of ligands and receptors in the membrane, as discussed by Bell, Dembo, and Bongrand [29,30]. Using phenomenological

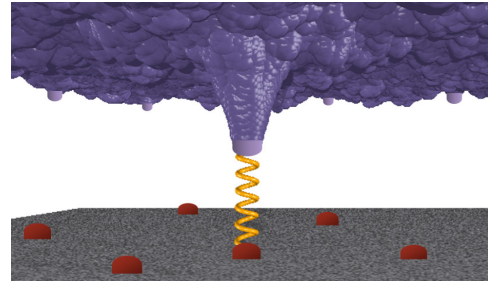


FIG. 1. Schematic representation of the system. The membrane (purple) that anchors receptors (yellow) fluctuates above the target surface. The membrane is locally deformed when the receptor forms a bond with the surface ligand (red).

arguments, they postulated that the unbinding rate depends on the force applied to the bond [29], while the binding rate was set to depend on the deformation energy of the bond, when the separation between the adherent surfaces is fixed [31]. Besides being used for modeling cell adhesion [29–32], these rate formulations have received numerous experimental support [21,33–36].

These rates were further modified in an *ad hoc* way to account for detailed balance and entropic considerations [32]. Such derivation leaves room for ambiguous interpretations of the normalizing factors, load-sharing coefficients, and the functional dependence on the intrinsic binding affinity, all of which were extensively discussed in the literature [37–39]. This ambiguity could be resolved by a first-principles derivation of the Bell-Dembo rates, which, from the start, accounts for the desired constraints such as detailed balance. Unfortunately, theoretical approaches to derive Bell-Dembo rates from first principles are still scarce. One attempt to derive the unbinding Bell rate was based on the Kramers' theory for the diffusive crossing of a model barrier in a simple free energy profile, first done in Refs. [40,41] and later in Refs. [42,43]. However, only irreversible bond breaking has been considered so far, which is, nonetheless, useful for the interpretation of single-molecule pulling experiments. However, this is not sufficient to describe the reversible binding associated with receptor-ligand interactions.

Over the last decades, further evidence was established that not only the average position of the membrane but also its roughness strongly affect the protein complexation rates [19,21,44–46]. To quantitatively study this relation, Bihl *et al.* [18,32] introduced the concept of coarse-grained (un)binding rates, which directly depend on the membrane fluctuation distribution [18,32]. The notion of coarse-grained (CG) rates has since been experimentally validated in mimetic [21] and cellular [22] systems, within the caveat of Gaussian noise and detailed balance.

However, there are several open issues with CG rates [18,32]. First of all, the CG rates are based on the phenomenological Bell-Dembo rates [29,31]. Second, the CG rate framework has been developed and tested only in

the context of thermal fluctuations. The effect of membrane activity on CG rates has not been studied so far, and it has not been clear how to generalize the CG rates to efficiently account for fluctuations that deviate from the purely thermal case. The main obstacle has been the idiosyncrasy of membrane driving mechanisms for different cell types and corresponding dynamical models that attempt to model the resulting membrane fluctuations.

The aim of this paper is therefore twofold. First, it gives a first-principles derivation of the Bell-Dembo rates by formulating a generic, analytical model that ensures detailed balance and takes into account the reversibility of the (un)binding process, thus deriving rates that validate Bell and Dembo's assumptions about the rate dependence on energy and force [21,32]. We follow up by integrating the derived Bell-like rates assuming Gaussian membrane fluctuations, thus deriving the Gaussian CG rates from first principles. Second, we extend our rate analysis to non-equilibrium conditions using an experimentally measured active-fluctuation spectrum. We first demonstrate that the height probability distributions of resting and activated human macrophages (HMs) and red blood cells (RBCs) can be modeled as a convolution of an asymmetric exponential and a Gaussian component, although their physiology and activation mechanisms are completely different. Hypothesising that this feature may be broadly relevant, we build a minimal mechanical model for this type of fluctuation spectrum. We derive the non-Gaussian CG rates, demonstrating the direct effect of fluctuations on the dynamics of binding. Finally, we show that rates can be cast into a universal form, irrespective of the timescales and of the nature (thermal or active) of membrane fluctuations.

II. SEPARATION OF TIMESCALES AND THE EFFECTIVE-RATES APPROACH

Our approach is motivated by a timescale separation between various degrees of freedom involved in ligand-receptor binding (Fig. 2). In the Kramer picture, the fundamental timescale for the binding and unbinding processes is defined by the height of the barrier between the bound and the unbound states. These barriers are functions of the protein conformation and membrane positions, setting the instantaneous rates k^+ and k^- (Fig. 2). Structural fluctuations of the membrane-protein system may appear as fluctuations in the heights of these barriers, which can be systematically integrated.

One starts with the fastest degrees of freedom—that of the proteins. Conformational changes of proteins may exhibit different characteristics with the reported timescales in the ps to 1- μ s regime [47] and may be triggered by an extracellular or intracellular stimulus or thermal excitations. Small structural fluctuations are fastest and occur on timescales of 10^{-15} – 10^{-12} s. On somewhat slower length scales, one encounters side chain flips (10^{-10} – 10^{-8} s) and then the domain motions (10^{-7} – 10^{-5} s). These motions

have to be delineated from larger secondary structure transformations which typically occur on slower timescales between 10^{-6} and 10^{-3} s. Some examples of these slow changes are allosteric transitions [48,49], cadherin catch bond lifetimes up to 10^{-2} s [50], or the spontaneous opening of the integrin on 1 μ s timescales [51].

The fastest degrees of freedom of the protein are several orders of magnitude faster than the fastest membrane fluctuation modes. We thus make an assumption that for each position of the membrane h , the receptor has time to explore all its available configurational space, enabling us to represent receptor fluctuations by an equilibrium probability distribution. A natural timescale k_0 appears, which is related to the free energy gain for creating a bond ϵ_b in an unconstrained ligand-receptor pair. As a result, one obtains rates k_{on} and k_{off} for a fixed membrane position, with all properties as suggested by Bell and Dembo. According to this approach, however, large, typically slow conformational changes of proteins should be treated as two populations of receptors as each conformer will have a specific size, elastic constant, affinity, and binding-pocket size.

In the next step (Fig. 2), one considers active and thermal membrane fluctuations as significantly faster than the bond kinetics. The characteristic timescales associated with the majority of active and thermal membrane fluctuation modes are within the range of 0.01–10 s [8]. For example, characteristic relaxation times of membrane fluctuations have been measured in red blood cells ($\tau = 0.1$ s) and macrophages ($\tau = 0.8$ s) [23]. This is consistent with timescales of active membrane processes, among which are fast protrusions and retractions due to the local (de)polymerization of individual actin filaments. Their association rate is estimated to be $k_{\text{on}} = 10$ (μM) $^{-1}$, which for typical actin concentrations of

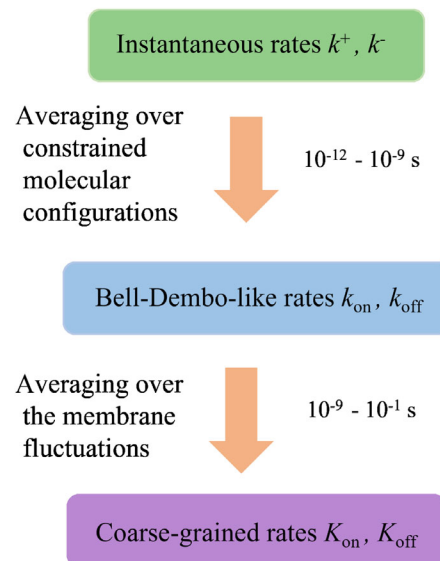


FIG. 2. Schematic representation of the rate averaging procedure and the relevant timescales in the system.

50 μM , gives $k_{\text{on}} = 5 \times 10^2 \text{ s}^{-1}$, while the dissociation rate is estimated to be $k_{\text{off}} = 1 \text{ s}^{-1}$ [52], falling into the 0.001–10 s interval [8]. It is these fluctuations that determine the probability for a membrane-anchored receptor and its target ligand to be within a binding range [20,53,54].

For unbinding, membrane fluctuations act as stochastic forces on already-formed bonds, promoting their breaking. Hence, Bell-Dembo rates, even when taking into account the mean membrane position, do not give an accurate estimate of the timescale on which the ligand-receptor (un)binding actually occurs. The effects of membrane fluctuations, nonetheless, can be integrated into coarse-grained rates K_{on} and K_{off} , under the assumption that the membrane explores its entire height distribution function prior to (un)binding.

The former assumption is well justified for the majority of biological ligand-receptor pairs. Namely, to justify the calculation of the unbinding rate K_{off} , it is instructive to discuss the weak ligand-receptor pairs for which the unbinding is more probable on shorter timescales than for stronger bonds. Thus, focusing on P-selectin, the dissociation rates $K_{\text{off}} = 1\text{--}10 \text{ s}^{-1}$ were reported in using flow chamber or adhesion experiments [33,35,36]. Therefore, the lower bound for the unbinding timescale of typical ligand-receptor pairs is estimated to be around 10^{-1} s . On the other hand, the majority of fluctuation modes of a bound membrane are expected to be faster than 10^{-1} s due to the suppression of slow membrane modes by the formed bond [55], ensuring that the membrane statistically explores available configurations before the unbinding event.

Similar arguments give justification to the integration of fluctuations into the binding rate K_{on} . Namely, typical values of the binding rates were estimated to be approximately 10^3 s^{-1} for the biotin-avidin bond (the strongest receptor-ligand bond found in nature, $E_b = 35k_B T$ [56]), approximately $10^0\text{--}10^1 \text{ s}^{-1}$ for integrin-RGD ($E_b = 10k_B T$), and approximately 10^{-1} s^{-1} for integrin-sialyl Lewis X ($E_b = 5k_B T$), as determined from growth models [20]. These estimates were done for radially expanding adhesions where the membrane is constrained to approximately 50 nm above receptors. This is why the reported timescale for biotin binding is several orders of magnitude larger than the timescale determined by fitting the Bell rate to the force-lifetime curve (approximately 10^{-10} s), when the binders are in close proximity.

First contacts between cells or of the cell with the extracellular matrix occur on even larger separations, and consequently, the rates for the initial bond formation are expected to be a couple orders of magnitude smaller than the rates for the formation of the following bonds. Hence, for typical adhesion receptors, the binding rate of the initial bond is estimated to be $K_{\text{on}} < 10^{-1} \text{ s}^{-1}$, or in terms of timescales, $\tau_{\text{on}} > 10 \text{ s}$, which is slower than the slowest membrane modes (approximately 1–10 s). Thus, the separation of timescales is a reasonable assumption, which is expected

to hold for typical cellular systems. Furthermore, the separation of timescales should also be valid for second and additional bonds, as both the binding rate and the relevant membrane timescales decrease simultaneously [55].

Note that our coarse-graining procedure does not account for the much slower remodeling of the global cellular shape, which is usually coupled to the significant remodeling of the cytoskeleton, which mechanically pushes the membrane and creates macroscopic protrusions. As the formation of membrane protrusion is an active, directed process, it requires a more complex regulation of the actin meshwork, involving the interaction of different proteins such as WASp, VASP, formin, or fascin [57]. Consequently, the membrane protrusion rates are within 1–2 $\mu\text{m}/\text{min}$ [58,59], much slower than the fast membrane fluctuations around the mean shape which are the focus of our coarse-graining procedure. However, such slow, global remodeling of the cellular shape can be accounted for by repeated calculation of the CG rates K_{on} and K_{off} for different cell shapes.

Although we have outlined the general recipe for calculating the CG rates, we still have to specify the exact form of the Bell-Dembo rates and the model for membrane fluctuations that would capture both the thermal and the active cases. We show a first-principles derivation of the Bell-Dembo rates in Sec. III, and we specify the membrane fluctuation models and average the Bell-Dembo rates into CG rates in Sec. IV. We show that the coarse-grained rates can also be cast in a simple Bell-like form, even in the presence of membrane activity, in Sec. V.

III. BELL-LIKE RATES FROM FIRST PRINCIPLES—THE ROLE OF RECEPTOR STRUCTURAL FLEXIBILITY

We start with a model system that consists of a target-ligand positioned at a distance h from a membrane with a receptor [Fig. 3(a)]. The target surface and the membrane are assumed to be immobile (we will tackle the problem of a fluctuating membrane later). We ignore the size of the ligand for simplicity. The receptor, on the other hand, has a finite size l_0 and is modeled as a fluctuating harmonic spring of stiffness λ . For convenience, we define $\lambda = \tilde{\lambda}/k_B T$, with Boltzmann constant k_B and temperature T , where $\tilde{\lambda}$ is in units of $k_B T/\text{length}^2$ and λ is in units $1/\text{length}^2$. The spring is anchored to the membrane at one end, and its tip is exploring the coordinate l .

This setup accounts for the fact that the structural fluctuations of the receptor happen on the ps- μs timescale [48,49], which is several orders of magnitude faster than the fastest membrane fluctuation modes. Thus, for all practical purposes, the membrane is stationary on these timescales. When the tip of the fluctuating receptor and the ligand are within a binding range, i.e., when the ligand is in the binding pocket of the receptor, they may form a bond. The pocket is modeled by a square well of width α , centered

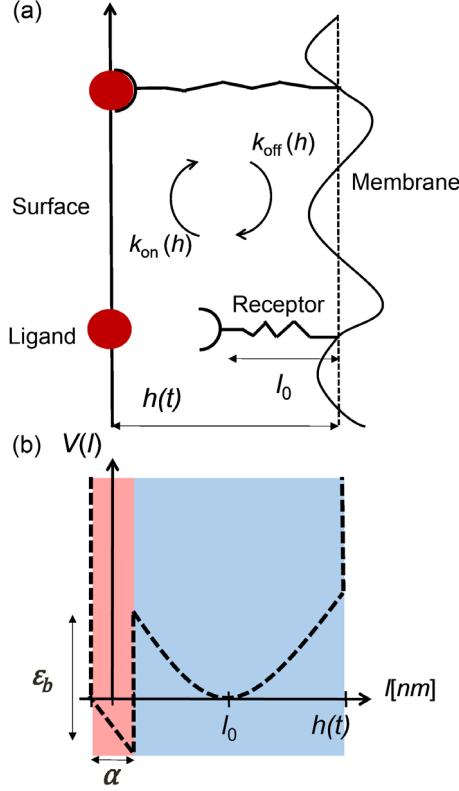


FIG. 3. Schematic representation of the model. (a) A receptor (spring) anchored to the membrane and the ligand (red circle) on the target surface. The surface and the membrane are separated by an instantaneous distance $h(t)$, which determines the binding rate $k_{\text{on}}(h)$ and the unbinding rate $k_{\text{off}}(h)$. (b) The model interaction potential (dashed line) between the ligand and the receptor. It consists of a harmonic potential centered at the position of the receptor's rest length $h - l_0$, shifted by a square well potential of width α and depth ϵ_b centered at the surface with the ligand. The red shaded area denotes the bound receptor state, while the blue shaded area denotes the unbound receptor state.

at the target, and a depth ϵ_b , denoting the intrinsic binding affinity of the pair. Again, for convenience, we define $\epsilon_b = \tilde{\epsilon}_b/k_B T$, where $\tilde{\epsilon}_b$ is in units of $k_B T$ and ϵ_b is dimensionless. The system therefore explores two states. The first is the unbound state forming with the rate $k_{\text{off}}(h)$, in which the receptor explores its conformational space independently of the ligand. The second state is the bound state forming with the rate $k_{\text{on}}(h)$, in which the receptor fluctuates within the binding pocket.

The internal energy of the system is captured by the dimensionless potential profile $V(l)$ [Fig. 3(b)],

$$V(l) = \begin{cases} \infty & \text{if } l \in (h, +\infty) \\ \frac{\lambda}{2}(l - (h - l_0))^2 & \text{if } l \in (\alpha/2, h] \\ \frac{\lambda}{2}(l - (h - l_0))^2 - \epsilon_b & \text{if } l \in [-\alpha/2, \alpha/2] \\ \infty & \text{if } l \in (-\infty, -\alpha/2). \end{cases} \quad (1)$$

Here, the origin of the coordinate system is set at the target surface [Fig. 3(a)]. The potential profile consists of a harmonic potential with minimum at $h - l_0$ (modeling receptor elasticity), shifted by ϵ_b in the interval $[-\alpha/2, \alpha/2]$. Positions $-\alpha/2$ and h are considered impermeable walls. The potential profile is naturally separated into two regions, representing the unbound state $u = (\alpha/2, h]$ and the bound state $b = [-\alpha/2, \alpha/2]$.

Given that the conformational changes of the protein are fast compared to the membrane, we assume that the receptor fluctuations reach thermal equilibrium for each membrane position. Hence, the probability distribution $p(l)$ for the position of the receptor tip l at some fixed h follows the Boltzmann distribution

$$p(l) = \frac{e^{-V(l)}}{\mathcal{Z}}, \quad \text{with } \mathcal{Z} = \int_{-\infty}^{\infty} dl e^{-V(l)}, \quad (2)$$

where \mathcal{Z} is the partition function of the system and $V(l)$ is the potential profile given in Eq. (1).

Under these circumstances, the rates $k_{\text{on}}(h)$ and $k_{\text{off}}(h)$ are given for a fixed membrane-target distance h by

$$k_{\text{on}}(h) = \frac{j(h)}{p_u(h)} \quad \text{and} \quad k_{\text{off}}(h) = \frac{j(h)}{p_b(h)}. \quad (3)$$

The subscript u denotes the unbound state and b the bound state, and $p_u(h)$ and $p_b(h)$ are thermal equilibrium probabilities of being in the respective states, while $j(h) \equiv |j_{u \rightarrow b}(h)| = |j_{b \rightarrow u}(h)|$ is the magnitude of the unidirectional current between the states in equilibrium, with $j_{u \rightarrow b}(h) = -j_{b \rightarrow u}(h)$.

The probabilities $p_u(h)$ and $p_b(h)$ are given by integrating the Boltzmann probability $p(l)$ over the corresponding regions of the states,

$$\begin{aligned} p_u(h) &= \frac{1}{\mathcal{Z}} \int_{\alpha/2}^h dl \exp \left[-\frac{\lambda}{2}(h - l - l_0)^2 \right] \\ &= \frac{1}{\mathcal{Z}} \sqrt{\frac{\pi}{2\lambda}} \left(\text{erf} \left[\sqrt{\lambda/2} l_0 \right] + \text{erf} \left[\sqrt{\lambda/2}(h - l_0 - \alpha/2) \right] \right) \\ &\approx \frac{1}{\mathcal{Z}} \sqrt{\frac{\pi}{2\lambda}} \left(\text{erf} \left[\sqrt{\lambda/2} l_0 \right] + \text{erf} \left[\sqrt{\lambda/2}(h - l_0) \right] \right), \end{aligned} \quad (4)$$

$$\begin{aligned} p_b(h) &= \frac{1}{\mathcal{Z}} \int_{-\alpha/2}^{\alpha/2} dl \exp \left[-\frac{\lambda}{2}(h - l - l_0)^2 + \epsilon_b \right] \\ &= \frac{1}{\mathcal{Z}} e^{\epsilon_b} \sqrt{\frac{\pi}{2\lambda}} \left(\text{erf} \left[\sqrt{\lambda/2}(h - l_0 + \alpha/2) \right] \right. \\ &\quad \left. - \text{erf} \left[\sqrt{\lambda/2}(h - l_0 - \alpha/2) \right] \right) \\ &\approx \frac{1}{\mathcal{Z}} \alpha \exp \left[-\frac{\lambda}{2}(h - l_0)^2 + \epsilon_b \right], \end{aligned} \quad (5)$$

where we assumed $\alpha/2 \ll h - l_0$ to expand the error functions. This is equivalent to stating that the binding pocket size α (angstrom scale) is much smaller than the distance between the target surface and the receptor rest position at $h - l_0$ (nanometer scale). The most important consequence of this reasonable approximation is that p_u is effectively independent of α while p_b is linear in α .

The current $j(h)$ is given by integrating over every path from state u to state b ,

$$j(h) \equiv |j_{u \rightarrow b}(h)| = \int_{\alpha/2}^{\infty} dl_u \int_{-\alpha/2}^{\alpha/2} dl_b p(l_u) k^+(l_u, l_b), \quad (6)$$

where $k^+(l_u, l_b)$ are the rates of transitions between any pair of microscopic states $l_u \in u$ and $l_b \in b$. Similarly, we can introduce the current $j_{b \rightarrow u}(h)$ that depends on $k^-(l_b, l_u)$, which are the rates of transitions from l_b to l_u . Given the equilibrium condition, detailed balance $k^+(l_u, l_b)/k^-(l_b, l_u) = \exp[\epsilon_b - (\lambda/2)(l_b - l_u)^2]$ must be satisfied. Hence, $|j_{u \rightarrow b}(h)| = |j_{b \rightarrow u}(h)|$, and it is enough to determine one of the two currents.

To proceed with the calculation of the current $j_{u \rightarrow b}(h)$, we assume that $k^+(l_u = \alpha/2, l_b) \gg k^+(l_u > \alpha/2, l_b)$; i.e., the microscopic rate for jumping in the binding pocket from the edge of the pocket is dominating all others, which is reasonable for steep harmonic potentials (stiff receptors). This leads to the assumption that only the path from position $\alpha/2$ in the state u to the state b contributes to the integral. We therefore set $k^+(l_u, l_b) = \delta(l_u - \alpha/2) \kappa^+ \times (l_u, l_b)$ (with Dirac delta δ) in Eq. (6) to find

$$j(h) = p(\alpha/2) \int_{-\alpha/2}^{\alpha/2} dl_b \kappa^+(\alpha/2, l_b). \quad (7)$$

Furthermore, we assume that the rate $\kappa^+(l_u = \alpha/2, l_b)$ for jumping from $\alpha/2$ to anywhere in the pocket is approximately constant, that is, $\kappa^+(l_u = \alpha/2, l_b) = k_0$, $\forall l_b$, where k_0 denotes some constant intrinsic rate. This is valid under the assumption that the binding pocket is small (typically a few angstroms) relative to the length scale of the receptor fluctuations (typically nanometers), which formally reads as $\alpha \ll \sqrt{2/\lambda}$. With this assumption, Eq. (7) becomes

$$j(h) = p(\alpha/2) k_0 \alpha. \quad (8)$$

Finally, by combining Eqs. (1)–(5) and (8), we find the h -dependent rates

$$k_{\text{on}}(h) = \frac{k_0 \alpha \sqrt{\frac{2\lambda}{\pi}} \exp[-\frac{\lambda}{2}(h - l_0 - \alpha/2)^2]}{\text{erf}[\sqrt{\lambda/2} l_0] + \text{erf}[\sqrt{\lambda/2}(h - l_0)]},$$

$$k_{\text{off}}(h) = k_0 \exp\left[-\epsilon_b + \frac{\alpha}{2} \left(\lambda \left(h - l_0 - \frac{\alpha}{4}\right)\right)\right]. \quad (9)$$

We note that a comparable expression for the binding rate was derived previously [60]. However, in that work, the unbinding rate was described independently with the Bell model, without constraining the rates to satisfy detailed balance. By assuming that the receptor fluctuation amplitude is small compared to the receptor size ($\sqrt{2/\lambda} \ll l_0 \rightarrow \text{erf}[l_0 \sqrt{\lambda/2}] \approx 1$) and compared to the distance between the receptor rest position and the target ($\sqrt{2/\lambda} \ll h - l_0 \rightarrow \text{erf}[(h - l_0) \sqrt{\lambda/2}] \approx 1$), the binding rate is further simplified, leading to

$$k_{\text{on}}(h) = k_0 \sqrt{\frac{\lambda \alpha^2}{2\pi}} \exp\left[-\frac{\lambda}{2} \left(h - l_0 - \frac{\alpha}{2}\right)^2\right], \quad (10)$$

$$k_{\text{off}}(h) = k_0 \exp\left[-\epsilon_b + \frac{\alpha}{2} \left(\lambda \left(h - l_0 - \frac{\alpha}{4}\right)\right)\right]. \quad (11)$$

Note that almost identical rates (up to a factor) were introduced in previous works [18,21,32] by physical reasoning but without formal derivation provided herein offering the exact criteria for the quality of these expressions. In short, the presented rates hold for stiff receptors ($\sqrt{1/\lambda} \ll l_0$) and small binding pockets ($\alpha \ll \sqrt{1/\lambda}$).

To give a physical interpretation of Eqs. (10) and (11), it is instructive to cast the rates in the following form:

$$k_{\text{on}}(h) = k_0 \exp[\Delta\sigma_u^b - W_{\langle u \rangle}^{u|b}], \quad (12)$$

$$k_{\text{off}}(h) = k_0 \exp[-\epsilon_b - W_{\langle b \rangle}^{u|b}], \quad (13)$$

where $\Delta\sigma_u^b = \sigma_b - \sigma_u = \ln \sqrt{(\lambda \alpha^2 / 2\pi k_B T)}$ is the entropic cost of restricting spring fluctuations to the binding pocket of width α , as also argued in recent work [32]. Furthermore, $W_{\langle u \rangle}^{u|b}$ is the work done against the spring force $f(l) = \lambda(l - (h - l_0))$ to stretch the receptor from its mean unbound position at $\langle u \rangle = h - l_0$ to the edge of the binding pocket $u|b = \alpha/2$,

$$W_{\langle u \rangle}^{u|b} = \int_{\langle u \rangle}^{u|b} dl f(l) = \int_{h-l_0}^{\alpha/2} dl \lambda(l - (h - l_0))$$

$$= \frac{\lambda}{2} \left(h - l_0 - \frac{\alpha}{2}\right)^2, \quad (14)$$

and $W_{\langle b \rangle}^{u|b}$ is the work done by the spring force on the path from the bound-state mean position in the absence of the force $\langle b \rangle = 0$ to the edge of the binding pocket $u|b = \alpha/2$,

$$\begin{aligned}
W_{\langle b \rangle}^{u|b} &= \int_{\langle b \rangle}^{u|b} dl f(l) = \int_0^{\alpha/2} d\lambda (l - (h - l_0)) \\
&= -\frac{\alpha}{2} \lambda \left(h - l_0 - \frac{\alpha}{4} \right). \quad (15)
\end{aligned}$$

The k_{on} rate depends exponentially on the work $W_{\langle u \rangle}^{u|b}$ needed to stretch the receptor from its mean unbound position at $h - l_0$ to the edge of the binding pocket $u|b = \alpha/2$, consistently with the phenomenological argument of Dembo [31]. As a result of the quadratic dependence in the exponent, the binding rate is highly sensitive to variations in target-membrane distance and receptor

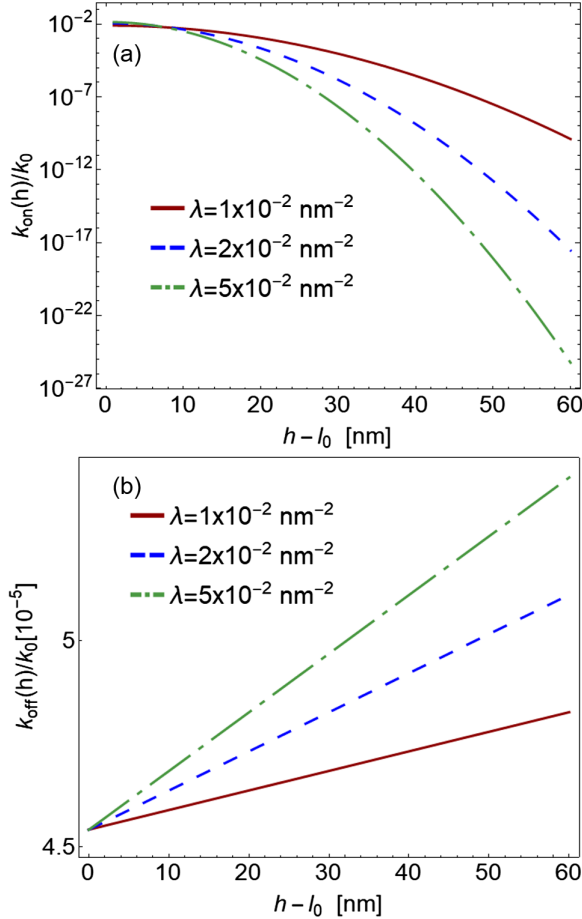


FIG. 4. Bell-like rates as a function of the distance between the ligand and the receptor for three different values of receptor stiffness λ . (a) Binding rate $k_{\text{on}}(h)$, given by Eq. (10) (b) Unbinding rate $k_{\text{off}}(h)$ given by Eq. (11). The width of the binding pocket is taken to be $\alpha = 0.2$ nm in both figures. The intrinsic binding affinity (depth of the potential well) is set to $\epsilon_b = 10$ ($k_B T$), as typical binding energies are within this range, e.g., $2 k_B T$ for E-cadherin interactions [61] and $35 k_B T$ for the biotin-streptavidin, which is the strongest bond found in nature [56]. Values for the receptor spring constants λ were motivated by prior work [62]. The intrinsic rate k_0 serves as an unspecified unit for the rates.

stiffness λ , spanning orders of magnitude for small variations in these parameters [Fig. 4(a)].

The unbinding rate $k_{\text{off}}(h)$ [Eq. (11)] depends exponentially on the binding pocket depth ϵ_b , diminished by the work $W_{\langle b \rangle}^{u|b}$ done by the spring force on the path from the bound-state mean position in the absence of the force $\langle b \rangle = 0$ to the edge of the binding pocket $u|b = \alpha/2$. By writing $W_{\langle b \rangle}^{u|b} = -\gamma \langle f(h) \rangle$, with $\gamma = \alpha/2$, we can interpret the unbinding rate $k_{\text{off}}(h)$ as depending exponentially on the product of the average force $\langle f(h) \rangle = (\int_{l_1}^{l_2} dl f(l; h)) / (l_1 - l_2)$ applied to the bond and a characteristic length γ of the bound-state microstructure, reproducing Bell's original assumption [29]

$$k_{\text{off}}(h) = k_0 \exp[-\epsilon_b + \gamma \langle f(h) \rangle]. \quad (16)$$

Bell reasoned that γ should be approximately the (half-) width of the binding pocket, which in our model is $\alpha/2$ and is exactly what we reproduced in Eq. (11). Note that the exact expression for the average force $\langle f(h) \rangle$ depends on the arbitrarily chosen position of the binding pocket (for example, it would be different for a binding pocket defined on $[-\alpha, 0]$ instead of $[-\alpha/2, \alpha/2]$), while the length γ depends only on the width and not the position of the pocket. Similarly, for the binding rate, the entropic term $\Delta\sigma_u^b$ depends only on the binding pocket width, while the exact expression for the deformation energy $W_{\langle u \rangle}^{u|b}$ depends on the pocket position. Because of the linear dependence of the unbinding rate exponent on h , $k_{\text{off}}(h)$ shows much less sensitivity to the separation from the target than the binding rate [Fig. 4(b)]. Notably, the intrinsic affinity ϵ_b appears only in the unbinding rate and does not enter the binding rate.

Variations of the Bell-Dembo rates in Eqs. (10) and (11) have often been used to fit the lifetime-force curves obtained from single-molecule force spectroscopy (SMFS) experiments, which enables determination of rate parameters, such as k_0 [43,63,64]. For example, by fitting Eq. (16) to lifetime-force data for a biotin-streptavidin bond, it is estimated that $\exp[\epsilon_b]/k_0 = 50$ hours [63]. For biotin-streptavidin, $\epsilon_b \approx 35 k_B T$ [56], resulting in the estimate $k_0 \approx 8 \times 10^9 \text{ s}^{-1}$. Based on the measurements of receptor-ligand binding rates in Ref. [20], we expect that typical adhesion molecules, such as integrins, have 2- to 4-orders-of-magnitude smaller k_0 than the biotin-streptavidin bond.

As a consistency check, we show that the ratio of rates satisfies a new detailed balance,

$$\frac{k_{\text{on}}(h)}{k_{\text{off}}(h)} = \exp[-W_{\langle u \rangle}^{u|b} + \epsilon_b + \Delta\sigma_u^b] \quad (17)$$

$$= \exp\left[-\frac{\lambda}{2}(h - l_0)^2 + \epsilon_b + \ln \sqrt{\frac{\lambda\alpha^2}{2\pi}}\right], \quad (18)$$

where the first term in the exponent on the right-hand side of Eq. (18) is $W_{\langle u \rangle}^{(b)} = W_{\langle u \rangle}^{u|b} - W_{\langle b \rangle}^{u|b} = W_{\langle u \rangle}^{u|b} + W_{u|b}^{(b)}$, the work needed to stretch the receptor spring from the mean unbound ($\langle u \rangle = h - l_0$) state to the mean bound state ($\langle b \rangle = 0$), stored in the elastic energy of the system. The second term is the intrinsic affinity ϵ_b , while the third term is the entropy cost associated with the suppression of the structural receptor fluctuations in the bound state [32]. As argued previously, the entropic term is necessary for a consistent mapping of the continuous configurational space to a coarse-grained space with two states (bound and unbound).

IV. COARSE-GRAINED RATES—THE EFFECT OF STEADY-STATE MEMBRANE FLUCTUATIONS

A. General integrative approach

As already discussed in Sec. II, the rates for a fixed target-membrane separation h do not give an accurate estimate of the timescale on which the ligand-receptor (un)binding actually occurs in the context of cell adhesion. Namely, fast membrane fluctuations often explore a range of different h before a single ligand-receptor (un)binding event occurs. Hence, estimating the timescale of ligand-receptor (un)binding in the context of cell adhesion by using rates [Eqs. (10) and (11)] for a specific h value will have poor accuracy. Instead, the observed separation of timescales between the ligand-receptor (un)binding and membrane fluctuations ($\tau_{\text{on/off}} > \tau_{\text{membrane}}$) allows us to assume that the membrane explores all available heights h [between the (un)binding events] and converges to a time-independent distribution [between the (un)binding events].

Actually, two h distributions are necessary—one for the unbound state [$p_u^{\text{mem}}(h)$] and one for the bound membrane [$p_b^{\text{mem}}(h)$] [18,32]. This is because the fluctuations in the membrane will be suppressed by the presence of the bond itself [55,65].

This enables us to calculate the effective rate $K_{\text{on/off}}$ as an expected value of the h -dependent rates $k_{\text{on/off}}(h)$ which quantify the timescale of the (un)binding events for the (fictive) case in which the membrane height is permanently at height h ,

$$K_{\text{on}} = \int dh k_{\text{on}}(h) p_u^{\text{mem}}(h), \quad (19)$$

$$K_{\text{off}} = \int dh k_{\text{off}}(h) p_b^{\text{mem}}(h). \quad (20)$$

Therefore, the assumption is that $k_{\text{on/off}}(h)$ contributes to the effective rate $K_{\text{on/off}}$ proportionally to the time the membrane spends at the height h .

These so-called CG rates depend only on the mechanical properties of the membrane-receptor system and the energy profile of the ligand-receptor interaction.

The above equations are general, in the sense that they hold for any time-independent h distributions. Two important classes of such distributions found in experiments are the equilibrium states (ES), for which the membrane is driven by purely thermal processes, and nonequilibrium steady states (NESS), which are generated in part by athermal biochemical processes requiring energy expenditure and, consequently, breaking the fluctuation-dissipation theorem [8]. Accordingly, it is not possible to distinguish an ES from a NESS based purely on the fluctuation measurements.

In the following section, we explore Gaussian distributions, which are important types of both ES and NESS h distributions. Because of their analytical tractability, Gaussian h distributions have already been extensively studied in the context of CG ligand-receptor rates [18,21,32]. After that, we examine a more general case of non-Gaussian distributions, inspired by the measurements of NESS fluctuations in HMs and RBCs. We exploit similarities in their NESS spectra to construct a single model for their fluctuations and then use Eqs. (19) and (20) to compare the two cases and analyze the consequences of non-Gaussianity for ligand-receptor interaction rates.

However, we should distinguish between the timescales of fast membrane fluctuations that we average into a time-independent distribution on intermediate timescales, and the much slower remodeling of the cell membrane, which changes its average shape and the fluctuation spectrum. As discussed previously, our approach assumes a quasistatic mean shape of the membrane and the fluctuation spectrum. Thus, to accurately apply our rate formulation in cell adhesion, the coarse-grained rates should be continuously updated, with the frequency of recalculation determined by the timescale of the remodeling.

B. Gaussian fluctuations: Thermal vs active systems

A Gaussian distribution of the membrane position h , with fluctuation amplitude $\sqrt{1/\lambda_G}$ and mean position h_0 , is given by

$$p_u^G(h) = \sqrt{\frac{\lambda_G}{2\pi}} \exp\left[-\frac{\lambda_G}{2}(h - h_0)^2\right]. \quad (21)$$

Note that in the ES case, the fluctuation amplitude $\sqrt{1/\lambda_G}$ depends on the membrane elastic properties, but it is independent of membrane deformation [65]. On the other hand, a membrane in an ES pinned by a linear spring with stiffness λ and rest length l_0 (see Fig. 5) has the following Gaussian distribution at the pinning site [65]:

$$p_b^G(h) = \sqrt{\frac{\lambda + \lambda_G}{2\pi}} \exp\left[-\frac{\lambda + \lambda_G}{2}(h - h_b)^2\right], \quad (22)$$

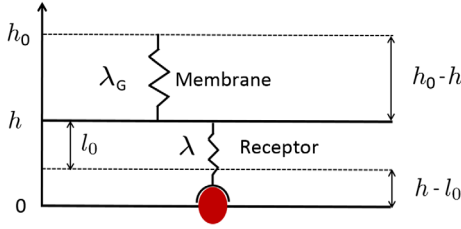


FIG. 5. Spring model of the interaction between a ligand and a receptor confined to a Gaussian membrane. The membrane is represented by a harmonic spring, with the rest position at h_0 . The receptor is represented by a harmonic spring of stiffness λ and rest length l_0 , which is coupled in series with the membrane spring. The ligand is represented by the red shape.

with the mean position

$$h_b = \frac{\lambda_G h_0 + \lambda l_0}{\lambda_G + \lambda} \quad (23)$$

and fluctuation amplitude $1/\sqrt{(\lambda + \lambda_G)}$.

We obtain the Gaussian CG rates according to Eqs. (19) and (20) by convolving the h -dependent reaction rates [Eqs. (10) and (11)] with the respective h distributions [Eqs. (21) and (22)], and we find

$$K_{\text{on}}^G = k_0 \sqrt{\frac{\Lambda_G \alpha^2}{2\pi}} \exp \left[-\frac{\Lambda_G}{2} \left(h_0 - l_0 - \frac{\alpha}{2} \right)^2 \right], \quad (24)$$

$$K_{\text{off}}^G = k_0 \exp \left[-\epsilon_b + \frac{\alpha}{2} \left(\Lambda_G \left(h_0 - l_0 - \frac{\alpha}{4} \right) \right) \right], \quad (25)$$

where $\Lambda_G = \lambda \lambda_G / (\lambda + \lambda_G)$ is the stiffness of the spring constructed by combining the membrane and receptor springs in series [21]. Remarkably, we can see from Eqs. (24) and (25) that the CG rates have exactly the same form as the Bell-like h -dependent rates [Eqs. (10) and (11)], with substitutions $h \rightarrow h_0$ and $\lambda \rightarrow \Lambda_G$.

In the limit of a very stiff membrane ($\lambda_G \rightarrow \infty$), the system is governed by the receptor flexibility ($\Lambda_G \rightarrow \lambda$), while in the limit of a very stiff receptor ($\lambda \rightarrow \infty$), the system is governed by the membrane flexibility ($\Lambda_G \rightarrow \lambda_G$). We can therefore map the membrane-receptor system to a simpler system consisting of a single, effective spring of stiffness Λ_G with rest length at $l = h_0 - l_0$, which binds and unbinds with Bell-like rates K_{on}^G and K_{off}^G from a binding pocket at $l = 0$ [18].

The interpretation of the CG rates is similar: K_{on}^G is proportional to the entropic cost of restraining both membrane and receptor fluctuations, and it depends exponentially on the energy needed to stretch the effective spring (membrane + receptor) to the edge of the binding pocket; K_{off}^G depends exponentially on the work done across the half-width of the pocket due to the deformation force of the effective spring (membrane + receptor). CG

rates inherit all of the properties discussed for the h -dependent Bell-like rates. Namely, the K_{on} rate is very sensitive to the changes in membrane fluctuations (through h_0 and Λ_G).

On the other hand, the K_{off} rate is less responsive. The reason behind this behavior comes from the fact that the exponent of K_{on}^G is quadratic in h_0 while the exponent of K_{off}^G is linear in h_0 . This was also shown in previous works [18,21,32], where Gaussian h distributions were used to calculate the CG rates K_{on} and K_{off} . This previous work validated the concept of effective reaction rates in the context of cell adhesion simulations by directly comparing the predictions of the CG approach with the higher-level simulation scheme that explicitly simulates the membrane fluctuations [32].

Finally, the detailed balance also holds on the level of a single bond and has the same form as Eq. (18), namely,

$$\frac{K_{\text{on}}^G}{K_{\text{off}}^G} = \exp \left[-\frac{\Lambda_G}{2} (h_0 - l_0)^2 + \epsilon_b + \ln \sqrt{\frac{\Lambda_G \alpha^2}{2\pi}} \right]. \quad (26)$$

The first term is due to elastic deformation of both the membrane and the receptor, the second term accounts for the intrinsic binding affinity, and the third term is the entropic cost of confining both membrane and receptor fluctuations to the binding pocket. The advantage of these rates is that they naturally coarse grain the dynamics of the receptor and the membrane while accurately resolving receptor-ligand reversible binding rates.

This formalism applies to ES but may also hold in a number of situations for a membrane exhibiting NESS Gaussian fluctuations. The condition is that the formation of the bond does not disturb the athermal processes that are driving the Gaussian NESS, on the timescale of unbinding. This is satisfied in many biological conditions; however, if not, (22) can still be safely calculated, while for the unbinding, the spectrum will need to be reevaluated.

C. Non-Gaussian active fluctuations and asymmetric environments

With contributions from active processes, the membrane fluctuation spectrum often delineates from a Gaussian distribution. This may have interesting consequences on the receptor-ligand (un)binding dynamics. We demonstrate this for non-Gaussian fluctuations that were experimentally measured on human macrophages [23] before and after the cell was stimulated (“primed”) with the cytokine IFN γ . Among other effects, IFN γ increases actin polymerization and membrane ruffling through the interplay with the membrane bound activators [26]. As a result of these nonequilibrium fluctuations, stronger excursions of the membrane are more common (Fig. 6), as can be seen by comparing the normalized spectra of activated (blue) and nonactivated (red) cells (see inset). Consequently, the

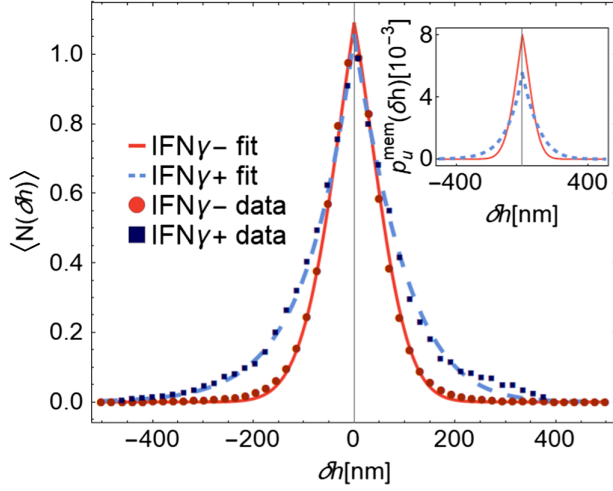


FIG. 6. Measurements of the change in stochastic displacements of a macrophage membrane in response to stimulation by the cytokine IFN γ . Membrane fluctuations of adhered macrophages were measured with dynamic optical displacement spectroscopy (DODS) [23]. Details about the preparation of macrophages and DODS can be found in Ref. [23]. Two distributions correspond to IFN γ -stimulated (red dots) and resting macrophages (blue dots). Lines are theoretical fits obtained using Eq. (27). Inset: probability distributions derived from the unnormalized fitted curves.

activation fattens the tails and lowers the peak of the NESS displacement distributions (see inset in Fig. 6).

Further analysis of these data shows that without IFN γ stimulation, the NESS displacements are slightly deviating from a Gaussian distribution (skewness $S = -0.09$ and excess kurtosis $K = 0.51$). Here, we use $S = E[((x - \mu)/\sigma)^3]$ as a measure of the skewness and excess kurtosis $K = E[((x - \mu)/\sigma)^4] - 3$ of the total distribution, with $E[x]$ being the expected value, μ the mean, and σ the standard deviation of the probability distribution. After IFN γ stimulation, the spectra are deviating more strongly from a Gaussian (skewness $S = -0.43$ and kurtosis $K = 2.05$). An increase in negative skewness indicates that activation increases asymmetry of the fluctuations by extending the tail for negative δh (towards the cell exterior) more than for positive δh (towards the cell interior), hinting at the asymmetry between the interior and the exterior membrane environments. To account for this effect, both the IFN γ -activated and the nonactivated measured distributions are fitted (Fig. 6) by

$$p_u^{GL}(h - h_0) = \frac{1}{Z_u^{GL}} \left\{ \exp \left[- \left(\frac{\lambda_{G^-}}{2} (h - h_0)^2 + \sqrt{\lambda_{L^-}} |h - h_0| \right) \right] \Theta(h_0 - h) + \exp \left[- \left(\frac{\lambda_{G^+}}{2} (h - h_0)^2 + \sqrt{\lambda_{L^+}} |h - h_0| \right) \right] \times \Theta(h - h_0) \right\}. \quad (27)$$

Here, λ_{G^+} and λ_{L^+} parametrize the Gaussian and Laplace distributed fluctuations toward the interior of the cell, respectively, as indicated by the Heaviside Θ function (positive $\delta h = h - h_0$). Equivalently, λ_{G^-} and λ_{L^-} account for the fluctuations toward the exterior of the cell (negative $\delta h = h - h_0$). Finally, Z_u^{GL} was taken as a free parameter in the fit; however, to convert the unnormalized fit to a proper probability distribution for further calculations, we take Z_u^{GL} to be the normalizing factor,

$$Z_u^{GL} = \sqrt{\frac{\pi}{2\lambda_{G^-}}} \exp \left[\frac{\lambda_{L^-}}{2\lambda_{G^-}} \right] \text{erfc} \left[\sqrt{\frac{\lambda_{L^-}}{2\lambda_{G^-}}} \right] + \sqrt{\frac{\pi}{2\lambda_{G^+}}} \exp \left[\frac{\lambda_{L^+}}{2\lambda_{G^+}} \right] \text{erfc} \left[\sqrt{\frac{\lambda_{L^+}}{2\lambda_{G^+}}} \right]. \quad (28)$$

The normalized distributions are plotted in the inset of Fig. 6.

For $\lambda_{L^\pm} \rightarrow 0$ and $\lambda_{G^+} \neq \lambda_{G^-}$, Eq. (27) reduces to an asymmetric Gaussian distribution, while for $\lambda_{G^\pm} \rightarrow 0$ and $\lambda_{L^+} \neq \lambda_{L^-}$, it reduces to an asymmetric Laplace distribution. At this stage, this form of the distribution does not imply the thermal or active nature of the (non-)Gaussian components, but it implies that membrane environments in the interior and the exterior are distinctively different. In the case that this is not true, it can be simply circumvented by setting $\lambda_{G^-} = \lambda_{G^+}$ and $\lambda_{L^-} = \lambda_{L^+}$, in which case, the usual symmetric distributions emerge.

One can understand the above distribution as the Boltzmann probability of an effective potential $V_{u^\pm}^{\text{eff}} = \lambda_{G^\pm}/2(h - h_0)^2 + \sqrt{\lambda_{L^\pm}}|h - h_0|$. Obviously, the potential $V_{u^\pm}^{\text{eff}}$ has an intuitive representation in the form of a parallel connection of a harmonic spring with stiffness λ_{G^\pm} and a linear spring with stiffness $\sqrt{\lambda_{L^\pm}}$. This system of springs will then be attached in series to a receptor (spring constant λ) as shown in Fig. 7. Under these circumstances, the

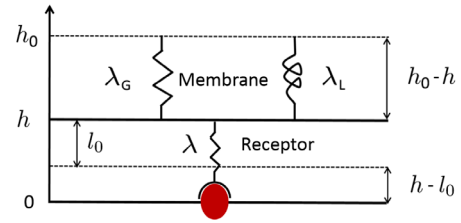


FIG. 7. Schematic representation of the mechanical model for binding rates of a ligand and receptor confined to an active membrane. The model consists of three coupled springs: one harmonic [deformation energy quadratic in extension, $\lambda_G(h - h_0)^2$] and the other linear [deformation energy linear in extension, $\sqrt{\lambda_L}|h - h_0|$], with the rest position of both springs at h_0 . The receptor is represented by a harmonic spring of stiffness λ and rest length l_0 , which is coupled in series with the parallel membrane springs.

normalizing factor Z_u^{GL} given in Eq. (28) can be interpreted as a partition function of the membrane-receptor coupled-springs system shown in Fig. 7.

Centering the data and applying Eq. (27) to the spectra of nonactivated macrophages in Fig. 6 yields parameter estimates $\lambda_{G^-} = 1.5 \times 10^{-4} \text{ nm}^{-2}$ and $\lambda_{L^-} = 8.2 \times 10^{-5} \text{ nm}^{-2}$ in the exterior, and $\lambda_{G^+} = 1.9 \times 10^{-4} \text{ nm}^{-2}$ and $\lambda_{L^+} = 5.2 \times 10^{-5} \text{ nm}^{-2}$ at the cell interior. The measurements on activated cells provide the values for the extracellular side $\lambda_{G^-} = 4.1 \times 10^{-6} \text{ nm}^{-2}$ and $\lambda_{L^-} = 1.1 \times 10^{-4} \text{ nm}^{-2}$, while on the cytoplasm side, one obtains $\lambda_{G^+} = 2.8 \times 10^{-6} \text{ nm}^{-2}$ and $\lambda_{L^+} = 7.9 \times 10^{-4} \text{ nm}^{-2}$. Cell activation clearly decreases λ_{G^\pm} and increases λ_{L^\pm} , confirming the strengthening of Laplace distributed fluctuations.

Interestingly, the Laplace component is significant even in the nonactivated cells, and the Gaussian component shows a notable level of asymmetry. While this finding can be interpreted as an indication that active fluctuations exist even in nonactivated macrophages, it is not a rigorous proof of the nonequilibrium state of these cells. However, given that these macrophages still consume energy, active components in the fluctuation spectrum of resting macrophages would not come as a surprise. Opposite to the finding in resting cells, in activated cells the Gaussian component has a smaller reach toward the extracellular space compared to that toward the cytosol, while the range of the Laplace fluctuations increases. These trends may have important consequences for the kinetics of receptors on the membrane surface.

Finally, we note that the same model has been successfully used to fit the active fluctuations of the RBCs (see Appendix A). RBCs and HMs have a very different molecular structure and activation mechanisms, yet the same trends in the relationship between cellular activity and membrane fluctuations are found. The presented Gauss-Laplace model is shown to correctly capture the main consequences of the cell activation on the membrane fluctuations for both cell types. Moreover, while RBCs do not adhere to the extracellular space, their membrane exhibits characteristic on/off coupling of the membrane-embedded glycoprotein with protein 4.1 of the intracellular spectrin network on the interior of the cell [28]. This is an adenosine triphosphate (ATP) dependent process, which may contribute to and couple with fluctuations. Therefore, we believe that the data on the RBC cell not only point to the similarities of fluctuation spectra in very different cell lines, but future models for the membrane-spectrin interaction may consider the coarse-graining concepts presented here.

1. Coarse-grained binding rate

We now turn to the consequences of the activated membrane fluctuations on the ligand-receptor binding and unbinding rates. Because the characteristic timescales

associated with the majority of active and thermal fluctuation modes are orders of magnitudes smaller than the timescale of ligand-receptor un(binding) [8,23] (see discussion in Sec. II), the averaging of Bell-like rates can be performed according to Eq. (19) using Eq. (27) to obtain the CG rate K_{on}^{GL} . Accordingly, inserting the h distribution $p_u^{GL}(h)$ into Eq. (19), we find, in the limit of a stiff receptor ($\lambda \gg \lambda_{G^\pm}, \lambda_{L^\pm}$ and $\sqrt{2/\lambda} \ll |h_0 - l_0|$) (see Appendix B. 1),

$$K_{\text{on}}^{GL} \approx \frac{k_0 \alpha}{Z_u^{GL}} \left\{ \exp \left[-h_\alpha^2 \frac{\lambda_{G^-}}{2} - h_\alpha \sqrt{\lambda_{L^-}} \right] \Theta[h_0 - l_0] + \exp \left[-h_\alpha^2 \frac{\lambda_{G^+}}{2} + h_\alpha \sqrt{\lambda_{L^+}} \right] \Theta[l_0 - h_0] \right\}, \quad (29)$$

where $h_\alpha = h_0 - l_0 - \alpha/2$. The above approximation is expected to be valid for most biological situations ($\lambda \sim 10^{-2} \text{ nm}^{-2}$ compared to $\lambda_{G^\pm}, \lambda_{L^\pm} \sim 10^{-6} - 10^{-3} \text{ nm}^{-2}$ from the above experimental fit). Note that $h_0 - l_0$ is defined as the relative position of the receptor tip with respect to the target-ligand positioned at the origin of the coordinate system and can therefore be positive or negative (see Fig. 7 for an example of positive $h_0 - l_0 > 0$). Equation (29) therefore tells us that the relative positioning of the membrane and the target ligand (the sign of $h_0 - l_0$) determines the side of the fluctuation spectrum that contributes to the ligand-receptor binding rate. If the target ligand is in the cell exterior ($h_0 - l_0 > 0$), the extracellular (negative) side of the spectrum will dominate interactions, while the intracellular (positive) side will contribute if the target ligand is in the cell interior ($h_0 - l_0 < 0$), as expected. Naturally, K_{on}^{GL} reduces to the symmetric Gaussian rate K_{on}^G [Eq. (24) in the regime $\lambda \gg \lambda_G$] for $\lambda_{G^-} = \lambda_{G^+}$ and $\lambda_{L^\pm} \rightarrow 0$.

In this picture, K_{on}^{GL} [Eq. (29)] depends exponentially on the effective energy needed to stretch both membrane springs to the edge of the binding pocket. Furthermore, it depends on the entropic cost $\ln[\alpha/Z_u^{GL}]$ of restraining fluctuations of both membrane springs, with partition function Z_u^{GL} , to the binding pocket of width α . We have therefore derived a generalized version of the binding rate for active systems in which the membrane fluctuations are exponentially and/or Gauss distributed. This result again inherits all of the main properties discussed for the h -dependent Bell-like binding rates. Namely, the K_{on}^{GL} rate is very sensitive to the changes in membrane fluctuations, which can modify the binding rate by orders of magnitude [Fig. 8(a)].

This sensitivity of rates becomes evident on the example of activated macrophages. Using the values of the membrane spring constants obtained from the fitted spectra, we test its effects on the binding rates in our model. We find that the binding rate decreases with increasing ligand-receptor distance $|h_0 - l_0|$, as expected. However, this decrease is much slower in the activated cells (blue lines in Fig. 8), compared to resting cells (red lines). The activation is thus reflected in the significantly extended

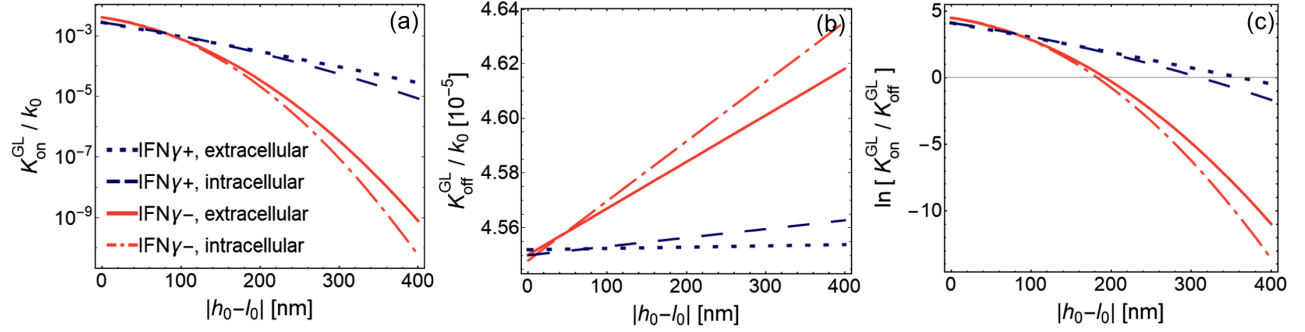


FIG. 8. Coarse-grained model for the ligand-receptor complexation in active (blue) and resting (red) macrophages as a function of the separation between the cell membrane and the target $h_0 - l_0$ on the extracellular (solid lines) and intracellular sides (dashed lines). (a) Binding rate $K_{\text{on}}^{\text{GL}}$ [Eq. (29)] is increased for orders of magnitude with activation, while the intracellular $K_{\text{on}}^{\text{GL}}$ is consistently smaller than the extracellular $K_{\text{on}}^{\text{GL}}$. (b) The unbinding rate $K_{\text{off}}^{\text{GL}}$ [Eq. (31)] decreases with activation, but the effect is only small. Nonetheless, the intracellular $K_{\text{off}}^{\text{GL}}$ is systematically larger than the extracellular $K_{\text{off}}^{\text{GL}}$. (c) The effective affinity $\ln[K_{\text{on}}^{\text{GL}} / K_{\text{off}}^{\text{GL}}]$ increases drastically with activation, and the decay in the bond stability as a function of the distance from the target is significantly slower in activated cells compared to resting cells, with the range of extracellular affinity being larger than the intracellular one. We use the parameters $\alpha = 0.5$ nm and $\epsilon_b = 10$. The values for λ_{G^\pm} and λ_{L^\pm} are taken from the experimental fits shown in Fig. 6. The intrinsic rate k_0 serves as an unspecified unit for the rates.

binding range. While the resting HM cell can realistically interact with receptors at a distance of about 250 nm, in activated cells this range is nearly doubled. This is presumably crucial in terms of the macrophage function. Furthermore, we notice that the asymmetry in fluctuations induces an asymmetry in rates. If the fluctuations involve binding to intracellular or extracellular targets, the rates for binding to intracellular targets (dashed lines) are consistently smaller than the rate for binding to extracellular targets (solid lines), and the range is about 50 nm less on the interior side, which is reasonable given the confinement of the cell.

These interesting properties fully emerge from the properties of the spectra. The form and the numerical values of the binding rate given in Eq. (29) are in no way dependent on the properties of the steady state. The result should be applicable as long as the Bell-Dezso rates can be considered, and the separation of timescales between the fluctuations of the membrane and the binding is still applicable.

The effect of membrane fluctuations on the binding rates can further be highlighted by a comparison with the case in which both the ligand and the receptor are anchored to immobile surfaces. Namely, receptor flexibility admits the receptor to explore the surrounding space only locally (about 10 nm), whereas membrane fluctuations can have amplitudes of about 100 nm. Consequently, in the absence of membrane fluctuations, the magnitude of the binding rate decreases by orders of magnitude (from $10^{-2}k_0$ to $10^{-12}k_0$) over just 30-nm distances (Fig. 4), whereas the presence of membrane fluctuations extends the comparable decrease of the binding rate over several hundreds of nm [Fig. 8(a)].

2. Coarse-grained unbinding rate

The formation of a bond typically affects the membrane height distribution $p_u^{\text{GL}}(h)$, as it locally constrains the

membrane movement. In order to calculate the coarse-grained unbinding rate $K_{\text{off}}^{\text{GL}}$, the height distribution function of a bound membrane is required. If we assume that the bond behaves as a thermalized elastic spring and that the fluctuations of the membrane can be represented by a convolution of Gauss and Laplace distributed displacements, the NESS distribution $p_b^{\text{GL}}(h)$ for the position h of a bound membrane can be written as

$$\begin{aligned}
 p_b^{\text{GL}}(h - h_0) &= \frac{1}{Z_b^{\text{GL}}} \exp \left[-\frac{\lambda}{2} (h - l_0)^2 \right] \\
 &\times \exp \left[-\left(\frac{\lambda_{G^-}}{2} (h - h_0)^2 + \sqrt{\lambda_{L^-}} |h - h_0| \right) \Theta(h_0 - h) \right] \\
 &\times \exp \left[-\left(\frac{\lambda_{G^+}}{2} (h - h_0)^2 + \sqrt{\lambda_{L^+}} |h - h_0| \right) \Theta(h - h_0) \right].
 \end{aligned} \tag{30}$$

In Eq. (30), we modeled the bond by a harmonic potential of stiffness λ and rest length l_0 as shown in Fig. 7, while Z_b^{GL} is the normalization constant.

To obtain the CG unbinding rate $K_{\text{off}}^{\text{GL}}$, we insert the h distribution in Eq. (30) into Eq. (20), and in the stiff receptor limit, we find (see Appendix B.2)

$$\begin{aligned}
 K_{\text{off}}^{\text{GL}} &\approx k_0 \exp \left[-\epsilon_b + \frac{\alpha}{2} \lambda_{G^-} \left(h_0 - l_0 - \frac{\alpha}{4} \right) + \frac{\alpha}{2} \sqrt{\lambda_{L^-}} \right] \\
 &\times \Theta[h_0 - l_0] \\
 &+ k_0 \exp \left[-\epsilon_b + \frac{\alpha}{2} \lambda_{G^+} \left(h_0 - l_0 - \frac{\alpha}{4} \right) - \frac{\alpha}{2} \sqrt{\lambda_{L^+}} \right] \\
 &\times \Theta[l_0 - h_0].
 \end{aligned} \tag{31}$$

Notably, the normalization constant drops out in this limit. Each theta function accounts for relative positioning of the membrane and the target ligand, with the sign of $h_0 - l_0$ determining if the bond is formed toward the interior or the exterior of the cell. The unbinding rate K_{off}^{GL} reduces to the symmetric Gaussian rate K_{off}^G [Eq. (25)] in the regime $\lambda \gg \lambda_G$ for $\lambda_{G^-} = \lambda_{G^+}$ and $\lambda_{L^\pm} \rightarrow 0$.

The calculated K_{off}^{GL} are shown in Fig. 8(b) as a function of the relative positioning between the target ligand and the membrane receptor ($|h_0 - l_0|$), for the case of macrophages. We find that, compared to the resting cells (red), the unbinding rates in activated cells are only slightly smaller, despite large changes in the spectra.

The interpretation of the rate given in Eq. (31) is analogous to the purely Gaussian case. Namely, K_{off}^{GL} depends exponentially on the work done across the half-width of the pocket due to the deformation force of both membrane springs (the force linear in extension is due to the harmonic spring, and the constant force is due to the linear spring). Note that the negative and positive sides of the rate are related through $h_0 - l_0 \rightarrow -(h_0 - l_0)$ and, importantly, $\alpha \rightarrow -\alpha$, where the sign in front of α indicates the orientation of the path over which the work is done ($[0, \alpha/2]$ for $h_0 - l_0 > 0$ and $[0, -\alpha/2]$ for $h_0 - l_0 < 0$). Hence, Eq. (31) represents a generalized version of the Bell-like unbinding rate. Moreover, this result follows from a very general assumption on the form of the probability distribution of a bound membrane [Eq. (30)] and the h -dependent rate $k_{\text{off}}(h)$ [Eq. (11)] and is therefore independent of the microscopic details and whether the receptor-membrane system is equilibrated or not.

As can be seen in Figs. 8(a) and 8(b), K_{off}^{GL} is insensitive to the changes in membrane fluctuations compared to the K_{on}^{GL} rate. The reason behind this behavior comes from the fact that the leading term in the exponent of K_{on}^{GL} is quadratic in membrane deformation, while the leading term in the exponent of K_{off}^{GL} is linear in deformation. This is remarkable since it follows that the Bell-like dependence of the unbinding rate on the load on the bond is present even in the effective picture, where the coarse graining is done over non-Gaussian fluctuations. This establishes a simple and unified framework for the investigation of the transmembrane receptor-ligand interactions.

In the context of macrophages, we see that the unbinding rate in activated cells (blue curves) is smaller compared to the rate in resting cells (red curves). In both cases, K_{off}^{GL} almost linearly increases by increasing the separation between the cell and the target, with the unbinding on the intracellular side being somewhat more intense than on the extracellular side.

In some systems, it will be possible to furthermore assume that, upon binding, the time-independent membrane fluctuation distribution is established on the time-scale of the bond lifetime, as it was in the case of thermal fluctuations. This is often a reasonable assumption since

the characteristic athermal fluctuation modes seem to be fast [8] compared to the lifetime of a bond [23]. If the ligand-receptor bond does not affect the internal structure of the membrane, nor the athermal processes that sustain the NESS, then the bond only mechanically constrains the movement of the membrane. In this case, the normalization constant in Eq. (30) can be interpreted as a partition function for the bound state. Moreover, the probability distribution of the membrane in the bound state is related to that in the unbound state such that in the limit of a very flexible receptor $\lambda \rightarrow 0$, the fluctuations are assumed to converge to the unbound membrane distribution $p_b^{GL}(h, \lambda = 0) = p_u^{GL}(h)$. Under these circumstances, detailed balance applies on the level of the single bond. Even for these types of active systems, however, having more than one bond will result in the breakdown of the detailed balance due to the membrane-mediated correlations [32].

3. Effective affinity for the receptor-ligand complexation in active membranes

The receptor-ligand affinity is given by the log ratio of the non-Gaussian binding and unbinding CG rates [Eqs. (29) and (31)]

$$\begin{aligned} \ln \frac{K_{\text{on}}^{GL}}{K_{\text{off}}^{GL}} = & \left(\epsilon_b - \frac{\lambda_{G^-}}{2} (h_0 - l_0)^2 - \sqrt{\lambda_{L^-}} (h_0 - l_0) \right. \\ & \left. + \ln \frac{\alpha}{Z_u^{GL}} \right) \Theta[h_0 - l_0] \\ & + \left(\epsilon_b - \frac{\lambda_{G^+}}{2} (h_0 - l_0)^2 + \sqrt{\lambda_{L^+}} (h_0 - l_0) \right. \\ & \left. + \ln \frac{\alpha}{Z_u^{GL}} \right) \Theta[l_0 - h_0]. \end{aligned} \quad (32)$$

The theta function terms again pick out the relevant side of the spectrum depending on the relative positioning of the target ligand and the membrane. The above non-Gaussian affinity has a simple interpretation analogous to the Gaussian case. Namely, the first term accounts for the enthalpic change in energy due to binding, the second and third are due to deformations of the membrane (represented by parallel springs), and the fourth term is the entropic cost of confining membrane fluctuations (represented by fluctuations of parallel springs) to the binding pocket of width α . In the special case of active systems that respect Boltzmann statistics, this relation can also be associated with the detailed balance condition.

If we apply this discussion to the physiologically induced changes in macrophage membrane fluctuations, we observe that fluctuations strongly affect the $K_{\text{on}}/K_{\text{off}}$ ratio, as K_{on} is much more sensitive to fluctuation changes than K_{off} [Fig. 8(c)]. This suggests that the activity of the cell may tune the affinity of receptors for their target.

Furthermore, the effect is present for interactions with both extracellular and intracellular structures, although it is more pronounced for the extracellular case. Furthermore, IFN γ activation extends the positive affinity to larger separations. This means that stable bonds can be established at separations that are 200 nm larger in the activated cells compared to resting cells, which is a considerable effect. As expected, the range of positive affinity is longer on the extracellular side, as a consequence of larger K_{on} and smaller K_{off} [Figs. 8(a) and 8(b)].

Hence, we predict that physiological changes in fluctuations can induce significant changes in the ligand-receptor binding dynamics and affinity. Based on that, we propose that the avidity of the macrophage receptors can be significantly modified, not only by changes in the receptor expression rate but also by physiologically controlling membrane fluctuations. Namely, the strengthening of adhesiveness is typically associated with the increase in receptor avidity, but the mechanisms for this increase are still highly debated [66]. Suggested mechanisms include cobinding, spatial distributions (which actually depend on fluctuations), production of receptors, and enhanced signaling, with probably more than one element contributing at the same time [67,68]. However, the biological community has not yet considered contributions from changes in membrane fluctuations. We hypothesize that this is a general mechanism across different types of cells for controlling the receptor-ligand-mediated membrane interactions, which would, e.g., enable macrophages to more effectively modify their phagocytic activity in the presence of pathogens.

Hence, understanding the activity-adhesiveness relation is an open problem and requires either decoupling of many possible contributions or approaching the problem holistically—starting from fluctuations themselves and not their auxiliary source, as performed here.

V. DISCUSSION

The generalized rate formulation.—We have introduced a systematic and unified framework for deriving and interpreting the kinetics and affinity of the adhesive receptor-ligand interactions in the context of both thermal and active fluctuations. This framework takes into account the physical properties of receptor-ligand bonds and the mechanics of the membrane and receptor shape fluctuations. Because of the characteristic timescales of these processes, it correctly describes the system behavior over several orders of magnitude on the temporal scale. Moreover, the framework is agnostic about the underlying mechanistic processes behind membrane activity and therefore on the exact types of cells under investigation (it should be applicable even to biomimetic vesicles, whatever the engineered mechanism of activity). This approach is also closer to the experimentalist point of view, as it explicitly considers only the observed fluctuation spectrum,

irrespective of its underlying driving mechanism, which is usually out of experimental reach.

Starting from a simple, yet physically reasonable microscopic model, we reproduced the qualitative behavior of Bell-Dembo rates; namely, the binding rate depends exponentially on the elastic energy needed to stretch the receptor in order to access the binding site, while the unbinding rate depends exponentially on the force exerted on the already-formed bond. In other words, expressed in terms of work, the binding rate depends exponentially on the work done by an external force that is exerted on the spring to stretch it from the spring rest length to the binding pocket, while the unbinding rate depends exponentially on the work done by the spring force on the path from the mean position in the binding pocket to the edge of the binding pocket. This is a general principle that can be used in modeling beyond the system described in this paper.

While Bell-like rates are extremely popular in the life-science community, they have so far been used with no clear understanding of the limits in which they apply and with no unambiguous interpretation of the normalization of the Boltzmann factors that appear. Our work here gives a clear interpretation of the latter and sets quantitative limits to the applicability of these rates—namely, for small binding pockets and stiff receptors, and when structural fluctuations of the receptor are faster than the binding. Furthermore, we give a more general expression, on the same level of theory, for any receptor stiffness [Eq. (9)].

Extending on these microscopic rates, we have calculated the CG rates that integrate membrane fluctuations. We reproduced the Gaussian rates and generalized them to the non-Gaussian case by modeling the membrane and the receptor system with an effective mechanical model. We found that even the non-Gaussian CG rates can be cast in the familiar Bell-like form. Consequently, we can define binding \mathcal{K}_{on} and unbinding \mathcal{K}_{off} rates, which may explicitly or implicitly depend on the separation between the membrane and the target h . These rates adopt the same form on all scales, namely,

$$\mathcal{K}_{\text{on}} = k_0 \exp[\Delta\sigma_u^b - W_{\langle u \rangle}^{u|b}], \quad (33)$$

$$\mathcal{K}_{\text{off}} = k_0 \exp[-\epsilon_b - W_{\langle b \rangle}^{u|b}]. \quad (34)$$

Here, $W_{\langle u \rangle}^{u|b}$ is the work done to deform the membrane-receptor construct from its (mean) unbound membrane-receptor distance $\langle u \rangle$ to bring the receptor to the edge of the binding pocket $u|b$, while $W_{\langle b \rangle}^{u|b}$ is the work done to deform the membrane-receptor construct to bring the receptor from the (mean) bound-state distance $\langle b \rangle$ (in the absence of the force) to the edge of the binding pocket $u|b$. Additionally, $\Delta\sigma_u^b = \sigma_b - \sigma_u$ is the entropic cost of restricting receptor fluctuations to the binding pocket. The only difference between the rates in Eqs. (12) and (13), Eqs. (24) and (25),

and Eqs. (29) and (31) is the mechanical model in question, namely, a single spring (a receptor alone) in Eqs. (12) and (13), two springs in series (a receptor and a Gaussian membrane) in Eqs. (24) and (25), or a construct of three springs (a receptor and a Gauss-Laplace membrane) in Eqs. (29) and (31). Consequently, all systems have in common that the target-membrane distance h enters the binding rate quadratically and the unbinding rate linearly.

Our approach therefore provides a “scale-free” formulation of rates. Importantly, the rates are given in terms of a measurable, load-dependent work function. Furthermore, the fact that such a work function can be formally derived from first principles in nonequilibrium conditions is a highly nontrivial result. Moreover, our framework indicates a simple way to account for the effects of membrane fluctuations even if their properties are not captured by the Gauss-Laplace model by corresponding modifications in the mechanical model of the receptor-membrane construct. Hence, the derived unified framework for passive and active fluctuations is a novel and positive result, which was not *a priori* obvious.

Furthermore, the Gaussian limit of our framework is already validated through the comparison of extensive simulations and experiments, especially on many-body processes such as adhesion [32]. Such investigations can now be effortlessly generalized to the non-Gaussian case. The degree of non-Gaussianity can be unambiguously controlled by modifying the model parameters, enabling systematic investigation of the non-Gaussianity effect. Moreover, the model is applicable for a large class of asymmetric non-Gaussian fluctuations that encompass Gaussian and Laplace distributions.

Finally, the rate formulation proposed in this paper can be applied in many different contexts, well beyond cell adhesion—from single-molecule force spectroscopy (when the ligands are attached to a fluctuating cantilever [69], or with antibody-antigen interactions studied with optical tweezers), in functional nanoparticle interactions during targeted delivery or in self-assembly, as well as in active soft-matter systems, just to name a few examples.

Beyond the single ligand-receptor pair.—Although the approach discussed in this work is based on a single ligand-receptor picture, our results already offer some insight into the membrane-mediated interactions between two receptor-ligand pairs. Namely, for Gaussian membrane fluctuations the membrane-mediated interactions between two bonds have been shown to be determined by the lateral correlation function of the unbound membrane [65]. The latter has, in turn, been shown to exhibit an exponential decay, with a characteristic lateral correlation length ξ_G , in the asymptotic limit of large separations between bonds [65]. Additionally, the lateral correlation length ξ_G can be shown to have a relatively simple relation to the fluctuation amplitude $1/\lambda_G$ [70]. In general, larger fluctuation amplitudes correspond to smaller lateral correlation lengths.

We expect that these general properties of the Gaussian fluctuations will also hold for the Gauss-Laplace fluctuations, with the caveat that the Gauss-Laplace membrane will be characterized by two lateral correlation lengths— ξ_G corresponding to the Gaussian contribution and ξ_L corresponding to the Laplace contribution—with the correlation length set by the larger of ξ_G and ξ_L .

With these assumptions, the experimental observation that $\lambda_G > \lambda_L$ before activation and $\lambda_G < \lambda_L$ after activation (see Sec. IV.C for exact values) translates into $\xi_G < \xi_L$ before activation and $\xi_G > \xi_L$ after activation. Therefore, the correlation length of the nonactivated macrophage fluctuations is expected to be set by the slower decaying Laplace contribution, while the correlation length for the activated fluctuations is set by the Gaussian contribution. Importantly, activation increases the correlation length, as the measured λ_G after activation is smaller than the λ_L before activation.

Hence, based on the above analysis of the single ligand-receptor model coupled with experimental fluctuation measurements, we expect that the activation will increase the range of membrane-mediated interactions. Such an effect can have important consequences for the clustering of ligand-receptor bonds in the context of adhesion and is in line with the hypothesis that membrane activity plays an important role in such processes. Namely, the correlation between activity and adhesiveness is an active field of study [24,25,71], and there are hints in the literature that fluctuations may indeed enhance adhesion. For example, Sengupta *et al.* [72] observed the time-resolved dynamics of spreading human neutrophils after activation by the chemoattractant formyl methionyl leucyl phenylalanine by reflection interference contrast microscopy. It was clearly seen that the cells have a “waiting period” without any visible adhesion or spreading before the chemoattractant was introduced—they start adhering only after that. Furthermore, immune cells have clearly shown the need for some kind of active fluctuations to establish early adhesion [73,74].

Of course, the discussion based on a single ligand-receptor pair picture is a rough estimate, and for the full treatment of the membrane-mediated interactions between bonds, one would have to specify a dynamical model that accounts for the activity. This would enable explicit calculation of the two-point correlation function for the active membrane and the investigation of the dependence of the macroscopic adhesion dynamics on the concentration of ligands and receptors, as was, for example, done in Ref. [75] for purely thermal dynamics. However, as already discussed, the specification of a dynamical model is a nontrivial task. This makes the simplicity and generality of the above analysis even more valuable. Moreover, any multibond model should contain, as its limit, the single-bond framework proposed here. Furthermore, the single ligand-receptor pair picture can be applied in modeling the

initial and intermediate stages of adhesion, where the separation between ligand-receptor pairs is larger than the correlation length of the membrane deformation. In the intermediate stages, activity certainly affects cooperativity by extending the correlation length between different receptor-ligand bonds; however, it is not safe to use the single pair approximation after the density of bonds increases too much. The low-density requirement can also be satisfied in biomimetic systems where the pattern of ligands on the adhesive surface can be experimentally controlled.

VI. CONCLUSIONS

The formalism developed in this paper paves the way for studies about the general interplay between non-Gaussian membrane fluctuations and processes such as bond domain formation, cell adhesion, phagocytosis, and cell motility. Our results show that, when the assumption of timescale separation is valid, the receptor-ligand rates can be estimated from the experimentally measured membrane fluctuations and the structural properties of the ligand-receptor pair. Importantly, it is not necessary to know the details of the underlying microscopic processes that are driving the membrane fluctuations, which was exemplified by the application of our method on HMs and RBCs. The shared qualitative features of their fluctuation spectra, before and after activation, motivated us to propose a single model for the spectra of their active fluctuations, although the underlying mechanism of activation was completely different. Moreover, the time independence of their spectra experimentally justified the averaging procedure of the ligand-receptor rates. Furthermore, we provided a genuine reinterpretation of the experimental data. Namely, we showed that the height probability distribution is consistent with a convolution of stochastic processes that are Gaussian and exponentially distributed. This was not previously appreciated in the literature (including in our own previous analysis). Moreover, this enables the mapping of the distribution to a mechanical spring model, which simplifies the analysis.

Using this insight, we showed that the asymmetry in amplitudes induces an asymmetry in rates. The rates for binding to intracellular targets are consistently smaller than the rates for binding to extracellular targets, and the range of fluctuation amplitudes is about 50 nm less on the interior side, which is reasonable given the confinement of the cell. The relative positioning of the membrane and target ligand determines the side of the fluctuation spectrum that contributes to the ligand-receptor binding rate.

In general, the binding rate decreases with increasing ligand-receptor distance. This decrease is much slower in the activated cells, compared to resting cells. The activation is thus reflected in the significantly extended binding range for the formation of the first bond, which is nearly doubled in an activated cell compared to the resting cell. Namely, to

form a stable initial bond, the average membrane-surface distance has to be on the order of the (half-)width of the unbound membrane fluctuations, which is approximately 200 nm for the nonactivated and approximately 400 nm for the activated macrophages (see Fig. 8).

Hence, we showed that physiological changes in fluctuations can induce significant changes in the ligand-receptor binding dynamics and affinity. Based on this result, we propose that this might be a mechanism present across different types of cells for controlling the receptor-ligand-mediated membrane interactions. We hope that further experimental investigations will validate the approach presented here and help to increase our understanding of cellularly regulated fluctuations and molecular binding kinetics.

ACKNOWLEDGMENTS

D. S. and J. A. J. were funded by European Research Council Starting Grant Membranes Act No. 337283. J. A. J. was supported in part by Croatian Science Foundation Project No. DOK-2018-01-9055. A.-S. S. and K. S. were funded by the joint German Science Foundation (DFG) and the French National Research Agency Project No. SM 289/8-1, AOBJ: 652939. A.-S. S. and R.M were funded by the Deutsche Forschungsgemeinschaft (DFG, German Research Foundation) Grant No. 363055819/GRK2415. D. S. was a member of the DFG funded RTG 1962 at the FAU Erlangen-Nurnberg. C. M. acknowledges financial support by the Volkswagen Foundation (Freigeist Fellowship, Project No. 94195) and DFG funded SFB1208 “Identity and dynamics of biological membranes” (Project No. 267205415).

A.-S. S. conceived the study and was in charge of the overall direction and supervision. U.S. helped shape the minimal model for the Bell rates and provided critical feedback on the entire work. C. M., R. M., and K.S provided experimental data. D. S. started on the analytical framework for the Bell-like rates. J. A. J. completed the calculation of the Bell-like rates, expanded the CG rate model for active membranes, and applied it to experimental data. A.-S. S. and J. A. J. wrote the manuscript with contributions from all authors.

APPENDIX A: RBC FLUCTUATIONS

To give an additional experimental argument for the general applicability of the active fluctuation model (27), we have repeated the analysis we used on the macrophage data, however, this time on the fluctuation data measured on RBCs [data taken from Ref. [23], Fig. 5(d)]. With RBCs, the role of the activator is played by the ATP molecules. The nonactivated RBCs are depleted of ATP, while the activation is done by adding the ATP to the solution. Note that RBCs exhibit spatially dependent fluctuations. For example, fluctuation amplitudes of 74 nm were measured at

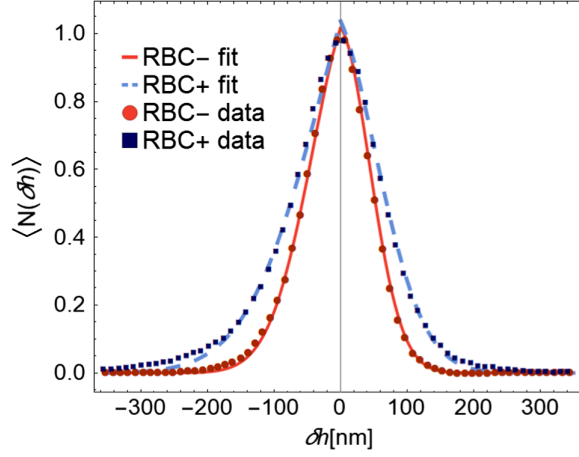


FIG. 9. Experimental data and the corresponding theoretical fits [Eq. (27)] of the RBC membrane fluctuations [23]. RBC- denotes the RBCs depleted of ATP, while RBC + denotes RBCs enriched with ATP. Negative δh correspond to the extracellular side of the distribution, while positive δh correspond to the intracellular side.

the thick rim, compared to the amplitudes of 41 nm in the center. Data presented in Fig. 9 are acquired after RBCs sedimented on a substrate, by measuring the fluctuations of the rim on the upper/distal membrane [23].

Along with the measured spectra in Fig. 9, one can see the corresponding fits [Eq. (27)]. Activation clearly

increases the tails of the distribution. It also observably increases the asymmetry, putting more weight on the negative (extracellular) part of the distribution. As can be seen, the fits capture the measurements well, both for the nonactivated and the activated case. The values of the fitted parameters show the same trend as observed with macrophages, namely, of increasing λ_L and decreasing λ_G with activation.

Specifically, the fit yields parameter estimates $\lambda_{G^-} = 2.3 \times 10^{-4} \text{ nm}^{-2}$ and $\lambda_{L^-} = 3.3 \times 10^{-5} \text{ nm}^{-2}$ at the cell exterior side, and $\lambda_{G^+} = 4.3 \times 10^{-4} \text{ nm}^{-2}$ and $\lambda_{L^+} = 4.8 \times 10^{-6} \text{ nm}^{-2}$ at the cell interior. The measurements on activated cells provide the values for the extracellular side $\lambda_{G^-} = 7.7 \times 10^{-5} \text{ nm}^{-2}$ and $\lambda_{L^-} = 4.7 \times 10^{-5} \text{ nm}^{-2}$, while on the cytoplasm side, one obtains $\lambda_{G^+} = 1.9 \times 10^{-4} \text{ nm}^{-2}$ and $\lambda_{L^+} = 1.7 \times 10^{-5} \text{ nm}^{-2}$. Hence, cell activation clearly decreases λ_{G^\pm} and increases λ_{L^\pm} , confirming the strengthening of Laplace distributed fluctuations, which reflect the slower decay of the distribution tails.

APPENDIX B: DERIVATION AND APPROXIMATION OF THE COARSE-GRAINED RATES

1. Binding rate

The partition function for the unbound state is given by $Z_u^{GL} = Z^+ + Z^-$, where

$$Z^\pm = \pm \int_0^{\pm\infty} dh \exp \left[-\frac{\lambda_{G^\pm}}{2} h^2 - \sqrt{\lambda_{L^\pm}} |h| \right] = \sqrt{\frac{\pi}{2\lambda_{G^\pm}}} \exp \left[\frac{\lambda_{L^\pm}}{2\lambda_{G^\pm}} \right] \text{erfc} \left[\sqrt{\frac{\lambda_{L^\pm}}{2\lambda_{G^\pm}}} \right]. \quad (\text{B1})$$

The coarse-grained binding rate K_{on}^{GL} is given by the convolution of the h distribution $p_u^{GL}(h)$ [Eq. (27)] with the h -dependent rate $k_{\text{on}}(h)$ [Eq. (10)], namely,

$$\begin{aligned} K_{\text{on}}^{GL} &= \int_{-\infty}^{\infty} dh k_{\text{on}}(h) p_u^{GL}(h - h_0) = \int_{-\infty}^{\infty} dh k_{\text{on}}(h + h_0) p_u^{GL}(h) \\ &= \frac{k_0 \alpha}{2Z_u^{GL}} \left\{ \frac{1}{\sqrt{1+G^-}} \exp \left[\frac{-h_\alpha^2 \lambda_{G^-} - 2h_\alpha \sqrt{\lambda_{L^-}} + L^-}{2(1+G^-)} \right] \text{erfc} \left[\frac{-h_\alpha \sqrt{\lambda} + \sqrt{L^-}}{\sqrt{2(1+G^-)}} \right] \right. \\ &\quad \left. + \frac{1}{\sqrt{1+G^+}} \exp \left[\frac{-h_\alpha^2 \lambda_{G^+} + 2h_\alpha \sqrt{\lambda_{L^+}} + L^+}{2(1+G^+)} \right] \text{erfc} \left[\frac{h_\alpha \sqrt{\lambda} + \sqrt{L^+}}{\sqrt{2(1+G^+)}} \right] \right\}, \end{aligned} \quad (\text{B2})$$

where $h_\alpha = h_0 - (l_0 + \alpha/2)$, $G^\pm = \lambda_{G^\pm}/\lambda$, and $L^\pm = \lambda_{L^\pm}/\lambda$. For $\lambda \gg \lambda_{G^\pm}, \lambda_{L^\pm}$, it follows that $G^\pm \rightarrow 0$ and $L^\pm \rightarrow 0$, and we find

$$K_{\text{on}}^{GL} \approx \frac{k_0 \alpha}{2Z_u^{GL}} \left\{ \exp \left[-h_\alpha^2 \frac{\lambda_{G^-}}{2} - h_\alpha \sqrt{\lambda_{L^-}} \right] \text{erfc} \left[\frac{-h_\alpha \sqrt{\lambda}}{\sqrt{2}} \right] + \exp \left[-h_\alpha^2 \frac{\lambda_{G^+}}{2} + h_\alpha \sqrt{\lambda_{L^+}} \right] \text{erfc} \left[\frac{h_\alpha \sqrt{\lambda}}{\sqrt{2}} \right] \right\}. \quad (\text{B3})$$

Furthermore, for $\sqrt{2/\lambda} \ll |h_\alpha|$, it follows that

$$\operatorname{erfc}\left[\frac{\pm h_\alpha \sqrt{\lambda}}{\sqrt{2}}\right] \approx \begin{cases} 0 & \text{if } \pm h_\alpha > 0 \\ 2 & \text{if } \pm h_\alpha < 0, \end{cases} \quad (\text{B4})$$

and we can further approximate Eq. (B3) with

$$K_{\text{on}}^{GL} \approx \frac{k_0 \alpha}{Z_u^{GL}} \left\{ \exp\left[-h_\alpha^2 \frac{\lambda_{G^-}}{2} - h_\alpha \sqrt{\lambda_{L^-}}\right] \Theta[h_\alpha] + \exp\left[-h_\alpha^2 \frac{\lambda_{G^+}}{2} + h_\alpha \sqrt{\lambda_{L^+}}\right] \Theta[-h_\alpha] \right\}. \quad (\text{B5})$$

Equation (29) follows by approximating the theta function arguments with $h_\alpha \approx h_0 - l_0$ (which is valid for small binding pockets $h_0 - l_0 \gg \alpha$).

2. Unbinding rate

The coarse-grained unbinding rate K_{off}^{GL} is given by the convolution of the h distribution $p_p^{GL}(h)$ [Eq. (27)] with the h -dependent rate $k_{\text{off}}(h)$ [Eq. (11)], namely,

$$\begin{aligned} K_{\text{off}}^{GL} &= \int_{-\infty}^{\infty} dh k_{\text{off}}(h) p_b^{GL}(h - h_0) = \int_{-\infty}^{\infty} dh k_{\text{off}}(h + h_0) p_b^{GL}(h) \\ &= k_0 \left\{ \frac{1}{1 + Z_b^+/Z_b^-} \exp\left[-\epsilon_b + \frac{(h_0 - l_0 - \alpha/4)\alpha\lambda_{G^-} + \alpha\sqrt{\lambda_{L^-}}}{2(1 + G^-)}\right] \frac{\operatorname{erfc}\left[\frac{-h_\alpha\sqrt{\lambda} + \sqrt{L^-}}{\sqrt{2(1+G^-)}}\right]}{\operatorname{erfc}\left[\frac{-(h_0-l_0)\sqrt{\lambda} + \sqrt{L^-}}{\sqrt{2(1+G^-)}}\right]} \right. \\ &\quad \left. + \frac{1}{1 + Z_b^-/Z_b^+} \exp\left[-\epsilon_b + \frac{(h_0 - l_0 - \alpha/4)\alpha\lambda_{G^+} - \alpha\sqrt{\lambda_{L^+}}}{2(1 + G^+)}\right] \frac{\operatorname{erfc}\left[\frac{h_\alpha\sqrt{\lambda} + \sqrt{L^+}}{\sqrt{2(1+G^+)}}\right]}{\operatorname{erfc}\left[\frac{(h_0-l_0)\sqrt{\lambda} + \sqrt{L^+}}{\sqrt{2(1+G^+)}}\right]} \right\}, \end{aligned} \quad (\text{B6})$$

where $h_\alpha = h_0 - (l_0 + \alpha/2)$, $G^\pm = \lambda_{G^\pm}/\lambda$, and $L^\pm = \lambda_{L^\pm}/\lambda$ and

$$\begin{aligned} Z_b^\pm &= \pm \int_0^{\pm\infty} dh \exp\left[-\frac{\lambda}{2}(h + (h_0 - l_0))^2 - \frac{\lambda_{G^\pm}}{2}h^2 - \sqrt{\lambda_{L^\pm}}|h|\right] \\ &= \sqrt{\frac{\pi}{2(\lambda + \lambda_{G^\pm})}} \exp\left[\frac{-\lambda\lambda_{G^\pm}(h_0 - l_0)^2 \pm 2(h_0 - l_0)\lambda\sqrt{\lambda_{L^\pm}} + \lambda_{L^\pm}}{2(\lambda + \lambda_{G^\pm})}\right] \operatorname{erfc}\left[\frac{\pm\lambda(h_0 - l_0) + \sqrt{\lambda_{L^\pm}}}{\sqrt{2(\lambda + \lambda_{G^\pm})}}\right]. \end{aligned} \quad (\text{B7})$$

For $h_0 - l_0 \gg \alpha$, we have $h_\alpha \approx h_0 - l_0$, and error functions in Eq. (B6) cancel out, leading to the following approximation:

$$K_{\text{off}}^{GL} \approx \frac{k_0}{1 + Z_b^+/Z_b^-} \exp\left[-\epsilon_b + \frac{(h_0 - l_0 - \alpha/4)\alpha\lambda_{G^-} + \alpha\sqrt{\lambda_{L^-}}}{2(1 + G^-)}\right] + \frac{k_0}{1 + Z_b^-/Z_b^+} \exp\left[-\epsilon_b + \frac{(h_0 - l_0 - \alpha/4)\alpha\lambda_{G^+} - \alpha\sqrt{\lambda_{L^+}}}{2(1 + G^+)}\right]. \quad (\text{B8})$$

Furthermore, the coefficients $1/(1 + Z^\pm/Z^\mp)$ for $\lambda \gg \lambda_{G^\pm}, \lambda_{L^\pm}$ and $\sqrt{2/\lambda} \ll |h_0 - l_0|$ behave in the following way:

$$\frac{1}{1 + Z^\pm/Z^\mp} \approx \begin{cases} 0 & \text{if } \pm(h_0 - l_0) < 0 \\ 1 & \text{if } \pm(h_0 - l_0) > 0, \end{cases} \quad (\text{B9})$$

which leads to the approximation

$$K_{\text{off}}^{GL} \approx k_0 \left(\exp\left[-\epsilon_b + \frac{(h_0 - l_0 - \alpha/4)\alpha\lambda_{G^-} + \alpha\sqrt{\lambda_{L^-}}}{2(1 + G^-)}\right] \Theta[h_0 - l_0] + \exp\left[-\epsilon_b + \frac{(h_0 - l_0 - \alpha/4)\alpha\lambda_{G^+} - \alpha\sqrt{\lambda_{L^+}}}{2(1 + G^+)}\right] \Theta[l_0 - h_0] \right). \quad (\text{B10})$$

Letting $G^\pm \rightarrow 0$ in the above equation, we arrive at Eq. (31).

- [1] C. Monzel, D. Schmidt, U. Seifert, A.-S. Smith, R. Merkel, and K. Sengupta, *Nanometric Thermal Fluctuations of Weakly Confined Biomembranes Measured with Microsecond Time-Resolution*, *Soft Matter* **12**, 4755 (2016).
- [2] P. Canham, *The Minimum Energy of Bending as a Possible Explanation of the Biconcave Shape of the Human Red Blood Cell*, *J. Theor. Biol.* **26**, 61 (1970).
- [3] W. Helfrich, *Elastic Properties of Lipid Bilayers: Theory and Possible Experiments*, *Z. Naturforsch.* **28C**, 693 (1973).
- [4] F. Brochard and J. F. Lennon, *Frequency Spectrum of the Flicker Phenomenon in Erythrocytes*, *J. Phys. France* **36**, 1035 (1975).
- [5] W. Helfrich and R.-M. Servuss, *Undulations, Steric Interaction and Cohesion of Fluid Membranes*, *Nuovo Cimento D* **3**, 137 (1984).
- [6] U. Seifert, *Configurations of Fluid Membranes and Vesicles*, *Adv. Phys.* **46**, 13 (1997).
- [7] T. Betz and C. Sykes, *Time Resolved Membrane Fluctuation Spectroscopy*, *Soft Matter* **8**, 5317 (2012).
- [8] H. Turlier, D. A. Fedosov, B. Audoly, T. Auth, N. S. Gov, C. Sykes, J.-F. Joanny, G. Gompper, and T. Betz, *Equilibrium Physics Breakdown Reveals the Active Nature of Red Blood Cell Flickering*, *Nat. Phys.* **12**, 513 (2016).
- [9] H. Turlier and T. Betz, *Fluctuations in Active Membranes*, in *Physics of Biological Membranes*, edited by P. Bassereau and P. Sens (Springer International Publishing, Cham, 2018), pp. 581–619.
- [10] J. Prost and R. Bruinsma, *Shape Fluctuations of Active Membranes*, *Europhys. Lett.* **33**, 321 (1996).
- [11] N. S. Gov and S. A. Safran, *Red Blood Cell Membrane Fluctuations and Shape Controlled by ATP-Induced Cytoskeletal Defects*, *Biophys. J.* **88**, 1859 (2005).
- [12] E. Ben-Isaac, Y. K. Park, G. Popescu, F. L. H. Brown, N. S. Gov, and Y. Shokef, *Effective Temperature of Red-Blood-Cell Membrane Fluctuations*, *Phys. Rev. Lett.* **106**, 238103 (2011).
- [13] P. Lenz, J.-F. Joanny, F. Jülicher, and J. Prost, *Membranes with Rotating Motors*, *Phys. Rev. Lett.* **91**, 108104 (2003).
- [14] N. Gov, *Membrane Undulations Driven by Force Fluctuations of Active Proteins*, *Phys. Rev. Lett.* **93**, 268104 (2004).
- [15] L. C.-L. Lin, N. Gov, and F. L. H. Brown, *Nonequilibrium Membrane Fluctuations Driven by Active Proteins*, *J. Chem. Phys.* **124**, 074903 (2006).
- [16] B. Loubet, U. Seifert, and M. A. Lomholt, *Effective Tension and Fluctuations in Active Membranes*, *Phys. Rev. E* **85**, 031913 (2012).
- [17] B. H. Stumpf, P. Nowakowski, C. Eggeling, A. Maciolek, and A.-S. Smith, *Protein Induced Lipid Demixing in Homogeneous Membranes*, *Phys. Rev. Research* **3**, L042013 (2021).
- [18] T. Bihl, U. Seifert, and A.-S. Smith, *Nucleation of Ligand-Receptor Domains in Membrane Adhesion*, *Phys. Rev. Lett.* **109**, 258101 (2012).
- [19] J. Hu, R. Lipowsky, and T. R. Weikl, *Binding Constants of Membrane-Anchored Receptors and Ligands Depend Strongly on the Nanoscale Roughness of Membranes*, *Proc. Natl. Acad. Sci. U.S.A.* **110**, 15283 (2013).
- [20] T. Bihl, S. Fenz, E. Sackmann, R. Merkel, U. Seifert, K. Sengupta, and A.-S. Smith, *Association Rates of Membrane-Coupled Cell Adhesion Molecules*, *Biophys. J.* **107**, L33 (2014).
- [21] S. Fenz, T. Bihl, D. Schmidt, R. Merkel, U. Seifert, K. Sengupta, and A.-S. Smith, *Membrane Fluctuations Mediate Lateral Interactions between Cadherin Bonds*, *Nat. Phys.* **13**, 906 (2017).
- [22] E. Toledo, G. L. Saux, A. Edri, L. Li, M. Rosenberg, Y. Keidar, V. Bhingardive, O. Radinsky, U. Hadad, C. D. Primo, T. Buffeteau, A.-S. Smith, A. Porgador, and M. Schwartzman, *Molecular-Scale Spatio-Chemical Control of the Activating-Inhibitory Signal Integration in NK Cells*, *Sci. Adv.* **7**, eabc1640 (2021).
- [23] C. Monzel, D. Schmidt, C. Kleusch, D. Kirchenbühler, U. Seifert, A.-S. Smith, K. Sengupta, and R. Merkel, *Measuring Fast Stochastic Displacements of Bio-membranes with Dynamic Optical Displacement Spectroscopy*, *Nat. Commun.* **6**, 8162 (2015).
- [24] T. D. Perez, M. Tamada, M. P. Sheetz, and W. J. Nelson, *Immediate-Early Signaling Induced by E-Cadherin Engagement and Adhesion*, *J. Biol. Chem.* **283**, 5014 (2008).
- [25] K. H. Biswas, K. L. Hartman, C. Yu, O. J. Harrison, H. Song, A. W. Smith, W. Y. C. Huang, W. Lin, Z. Guo, A. Padmanabhan, S. M. Troyanovsky, M. L. Dustin, L. Shapiro, B. Honig, R. Zaidel-Bara, and J. T. Groves, *E-Cadherin Junction Formation Involves an Active Kinetic Nucleation Process*, *Proc. Natl. Acad. Sci. U.S.A.* **112**, 10932 (2015).
- [26] K. Schroder, P. J. Hertzog, T. Ravasi, and D. A. Hume, *Interferon-Gamma: An Overview of Signals, Mechanisms and Functions*, *J. Leukoc. Biol.* **75**, 163 (2004).
- [27] D. Erbe, J. Collins, L. Shen, R. Graziano, and M. Fanger, *The Effect of Cytokines on the Expression and Function of Fc Receptors for IgG on Human Myeloid Cells*, *Molecular Immunology* **27**, 57 (1990).
- [28] Y. Park, C. A. Best, T. Auth, N. S. Gov, S. A. Safran, G. Popescu, S. Suresh, and M. S. Feld, *Metabolic Remodeling of the Human Red Blood Cell Membrane*, *Proc. Natl. Acad. Sci. U.S.A.* **107**, 1289 (2010).
- [29] G. Bell, *Models for the Specific Adhesion of Cells to Cells*, *Science* **200**, 618 (1978).
- [30] G. I. Bell, M. Dembo, and P. Bongrand, *Cell Adhesion. Competition between Nonspecific Repulsion and Specific Bonding*, *Biophys. J.* **45**, 1051 (1984).
- [31] M. Dembo, D. Torney, K. Saxman, and D. Hammer, *The Reaction-Limited Kinetics of Membrane-to-Surface Adhesion and Detachment*, *Proc. R. Soc. B* **234**, 55 (1988).
- [32] T. Bihl, U. Seifert, and A.-S. Smith, *Multiscale Approaches to Protein-Mediated Interactions between Membranes-Relating Microscopic and Macroscopic Dynamics in Radially Growing Adhesions*, *New J. Phys.* **17**, 083016 (2015).
- [33] R. Alón, D. A. Hammer, and T. A. Springer, *Lifetime of the P-Selectin-Carbohydrate Bond and Its Response to Tensile Force in Hydrodynamic Flow*, *Nature (London)* **374**, 539 (1995).
- [34] R. Merkel, P. Nassoy, A. Leung, K. Ritchie, and E. Evans, *Energy Landscapes of Receptor-Ligand Bonds Explored with Dynamic Force Spectroscopy*, *Nature (London)* **397**, 50 (1999).

- [35] S. Chen and T.A. Springer, *Selectin Receptor-Ligand Bonds: Formation Limited by Shear Rate and Dissociation Governed by the Bell Model*, *Proc. Natl. Acad. Sci. U.S.A.* **98**, 950 (2001).
- [36] B. T. Marshall, M. Long, J. W. Piper, T. Yago, R. P. McEver, and C. Zhu, *Direct Observation of Catch Bonds Involving Cell-Adhesion Molecules*, *Nature (London)* **423**, 190 (2003).
- [37] U. Seifert, *Dynamic Strength of Adhesion Molecules: Role of Rebinding and Self-Consistent Rates*, *Europhys. Lett.* **58**, 792 (2002).
- [38] P. Robert, K. Sengupta, P.-H. Puech, P. Bongrand, and L. Limozin, *Tuning the Formation and Rupture of Single Ligand-Receptor Bonds by Hyaluronan-Induced Repulsion*, *Biophys. J.* **95**, 3999 (2008).
- [39] R. Blackwell, D. Jung, M. Bukenberger, and A.-S. Smith, *The Impact of Rate Formulations on Stochastic Molecular Motor Dynamics*, *Sci. Rep.* **9**, 18373 (2019).
- [40] E. Evans and K. Ritchie, *Dynamic Strength of Molecular Adhesion Bonds*, *Biophys. J.* **72**, 1541 (1997).
- [41] S. Izrailev, S. Stepaniants, M. Balsera, Y. Oono, and K. Schulten, *Molecular Dynamics Study of Unbinding of the Avidin-Biotin Complex*, *Phys. Rev. Lett.* **72**, 1568 (1997).
- [42] O. K. Dudko, G. Hummer, and A. Szabo, *Intrinsic Rates and Activation Free Energies from Single-Molecule Pulling Experiments*, *Phys. Rev. Lett.* **96**, 108101 (2006).
- [43] O. K. Dudko, G. Hummer, and A. Szabo, *Theory, Analysis, and Interpretation of Single-Molecule Force Spectroscopy Experiments*, *Proc. Natl. Acad. Sci. U.S.A.* **105**, 15755 (2008).
- [44] T. R. Weikl, M. Asfaw, H. Krobath, B. Rózycki, and R. Lipowsky, *Adhesion of Membranes via Receptor-Ligand Complexes: Domain Formation, Binding Cooperativity, and Active Processes*, *Soft Matter* **5**, 3213 (2009).
- [45] E. Reister, T. Bihl, U. Seifert, and A.-S. Smith, *Two Intertwined Facets of Adherent Membranes: Membrane Roughness and Correlations between Ligand-Receptors Bonds*, *New J. Phys.* **13**, 025003 (2011).
- [46] S. F. Fenz, T. Bihl, R. Merkel, U. Seifert, K. Sengupta, and A.-S. Smith, *Switching from Ultraweak to Strong Adhesion*, *Adv. Mater.* **23**, 2622 (2011).
- [47] R. O. Dror, R. M. Dirks, J. Grossman, H. Xu, and D. E. Shaw, *Biomolecular Simulation: A Computational Microscope for Molecular Biology*, *Annu. Rev. Biophys.* **41**, 429 (2012).
- [48] F. Musiani, G. Rossetti, L. Capece, T. M. Gerger, C. Micheletti, G. Varani, and P. Carloni, *Molecular Dynamics Simulations Identify Time Scale of Conformational Changes Responsible for Conformational Selection in Molecular Recognition of HIV-1 Transactivation Responsive RNA*, *J. Am. Chem. Soc.* **136**, 15631 (2014).
- [49] K. El Hage, S. Brickel, S. Hermelin, G. Gaulier, C. Schmidt, L. Bonacina, S. C. van Keulen, S. Bhattacharyya, M. Chergui, P. Hamm, U. Rothlisberger, J.-P. Wolf, and M. Meuwly, *Implications of Short Time Scale Dynamics on Long Time Processes*, *Struct. Dyn.* **4**, 061507 (2017).
- [50] K. Manibog, H. Li, S. Rakshit, and S. Sivasankar, *Resolving the Molecular Mechanism of Cadherin Catch Bond Formation*, *Nat. Commun.* **5**, 3941 (2014).
- [51] W. Chen, J. Lou, J. Hsin, K. Schulten, S. C. Harvey, and C. Zhu, *Molecular Dynamics Simulations of Forced Unbending of Integrin $\alpha_v\beta_3$* , *PLoS Comput. Biol.* **7**, e1001086 (2011).
- [52] J. R. Kuhn and T. D. Pollard, *Real-Time Measurements of Actin Filament Polymerization by Total Internal Reflection Fluorescence Microscopy*, *Biophys. J.* **88**, 1387 (2005).
- [53] Y. Wu, J. Vendome, L. Shapiro, A. Ben-Shaul, and B. Honig, *Transforming Binding Affinities from Three Dimensions to Two with Application to Cadherin Clustering*, *Nature (London)* **475**, 510 (2011).
- [54] L. Ju, J. Qian, and C. Zhu, *Transport Regulation of Two-Dimensional Receptor-Ligand Association*, *Biophys. J.* **108**, 1773 (2015).
- [55] J. A. Janeš, D. Schmidt, R. Blackwell, U. Seifert, and A.-S. Smith, *Statistical Mechanics of an Elastically Pinned Membrane: Equilibrium Dynamics and Power Spectrum*, *Biophys. J.* **117**, 542 (2019).
- [56] C. A. Helm, W. Knoll, and J. N. Israelachvili, *Measurement of Ligand-Receptor Interactions*, *Proc. Natl. Acad. Sci. U.S.A.* **88**, 8169 (1991).
- [57] C. Schäfer, B. Borm, S. Born, C. Möhl, E.-M. Eibl, and B. Hoffmann, *One Step Ahead: Role of Filopodia in Adhesion Formation During Cell Migration of Keratinocytes*, *Exp. Cell Res.* **315**, 1212 (2009).
- [58] D. Garbett, A. Bisaria, C. Yang, D. G. McCarthy, A. Hayer, W. E. Moerner, T. M. Svitkina, and T. Meyer, *T-Plastin Reinforces Membrane Protrusions to Bridge Matrix Gaps During Cell Migration*, *Nat. Commun.* **11**, 4818 (2020).
- [59] H. Shafqat-Abbasi, J. M. Kowalewski, A. Kiss, X. Gong, P. Hernandez-Varas, U. Berge, M. Jafari-Mamaghani, J. G. Lock, and S. Strömblad, *An Analysis Toolbox to Explore Mesenchymal Migration Heterogeneity Reveals Adaptive Switching between Distinct Modes*, *eLife* **5**, e11384 (2016).
- [60] T. Erdmann and U. S. Schwarz, *Impact of Receptor-Ligand Distance on Adhesion Cluster Stability*, *Eur. Phys. J. E* **22**, 123 (2007).
- [61] S. Sivasankar, W. Briehner, N. Lavrik, B. Gumbiner, and D. Leckband, *Direct Molecular Force Measurements of Multiple Adhesive Interactions between Cadherin Ectodomains*, *Proc. Natl. Acad. Sci. U.S.A.* **96**, 11820 (1999).
- [62] I. Kosztin, R. Bruinsma, P. O’Lague, and K. Schulten, *Mechanical Force Generation by G Proteins*, *Proc. Natl. Acad. Sci. U.S.A.* **99**, 3575 (2002).
- [63] S. Gruber, A. Löf, S. M. Sedlak, M. Benoit, H. E. Gaub, and J. Lipfert, *Designed Anchoring Geometries Determine Lifetimes of Biotin-Streptavidin Bonds under Constant Load and Enable Ultra-Stable Coupling*, *Nanoscale* **12**, 21131 (2020).
- [64] R. W. Friddle, A. Noy, and J. D. Yoreo, *Interpreting the Widespread Nonlinear Force Spectra of Intermolecular Bonds*, *Proc. Natl. Acad. Sci. U.S.A.* **109**, 13573 (2012).
- [65] J. A. Janeš, H. Stumpf, D. Schmidt, U. Seifert, and A.-S. Smith, *Statistical Mechanics of an Elastically Pinned Membrane: Static Profile and Correlations*, *Biophys. J.* **116**, 283 (2019).
- [66] N. Ni, C. G. Kevil, D. C. Bullard, and D. F. Kucik, *Avidity Modulation Activates Adhesion under Flow and Requires*

- Cooperativity among Adhesion Receptors*, *Biophys. J.* **85**, 4122 (2003).
- [67] M. Sanchez-Lockhart, A. V. Rojas, M. M. Fettes, R. Bauserman, T. R. Higa, H. Miao, R. E. Waugh, and J. Miller, *T Cell Receptor Signaling Can Directly Enhance the Avidity of CD28 Ligand Binding*, *PLoS One* **9**, e89263 (2014).
- [68] B. E. Bierer and W. C. Hahn, *T Cell Adhesion, Avidity Regulation and Signaling: A Molecular Analysis of CD2*, *Seminars in immunology* **5**, 249 (1993).
- [69] M. Nguyen-Duong, K. W. Koch, and R. Merkel, *Surface Anchoring Reduces the Lifetime of Single Specific Bonds*, *Europhys. Lett.* **61**, 845 (2003).
- [70] J. Rädler, T. Feder, H. Strey, and E. Sackmann, *Fluctuation Analysis of Tension-Controlled Undulation Forces between Giant Vesicles and Solid Substrates*, *Phys. Rev. E* **51**, 4526 (1995).
- [71] E. Bazellières, V. Conte, A. Elosegui-Artola, X. Serra-Picamal, M. Bintanel-Morcillo, P. Roca-Cusachs, J. J. Muñoz, M. Sales-Pardo, R. Guimerà, and X. Trepac, *Control of Cell-Cell Forces and Collective Cell Dynamics by the Intercellular Adhesome*, *Nat. Cell Biol.* **17**, 409 (2015).
- [72] K. Sengupta, H. Aranda-Espinoza, L. Smith, P. Janmey, and D. Hammer, *Spreading of Neutrophils: From Activation to Migration*, *Biophys. J.* **91**, 4638 (2006).
- [73] A. Pierres, A.-M. Benoliel, D. Touchard, and P. Bongrand, *How Cells Tiptoe on Adhesive Surfaces Before Sticking*, *Biophys. J.* **94**, 4114 (2008).
- [74] E. Cai, K. Marchuk, P. Beemiller, C. Beppler, M. G. Rubashkin, V. M. Weaver, A. Gérard, T.-L. Liu, B.-C. Chen, E. Betzig, F. Bartumeus, and M. F. Krümmel, *Visualizing Dynamic Microvillar Search and Stabilization During Ligand Detection by T Cells*, *Science* **356**, eaal3118 (2017).
- [75] H. Krobath, B. Rózycki, R. Lipowsky, and T. R. Weikl, *Binding Cooperativity of Membrane Adhesion Receptors*, *Soft Matter* **5**, 3354 (2009).